Asymptotic behavior of a degenerate forest kinematic model with a perturbation

Lu Li, Guillaume Cantin

Asymptotic behavior of a degenerate forest kinematic model with a perturbation

Lu LI[*], Guillaume Cantin[†]

June 12, 2024

Abstract

In this paper, we study the asymptotic behavior of the global solutions to a degenerate forest kinematic model, under the action of a perturbation modelling the impact of climate change. In the case where the main nonlinear term of the model is monotone, we prove that the global solutions converge to a stationary solution, by showing that the Lyapunov function deduced from the system satisfies a Łojasiewicz-Simon gradient inequality. We also present an original algorithm, based on the Statistical Model Checking framework, to estimate the probability of convergence towards non-constant equilibria. Furthermore, under suitable assumptions on the parameters, we prove the continuity of the flow and of the stationary solutions with respect to the perturbation parameter. Then, we succeed in proving the robustness of the weak attractors, by considering a weak topology phase space and establishing the existence of a family of positively invariant regions. At last, we present numerical simulations of the model and experiment the behavior of the solutions under the effect of several types of perturbations. We also show that the forest kinematic model can lead to the emergence of chaotic patterns.

Key words. Forest kinematic model, perturbation, asymptotic behavior, Łojasiewicz-Simon gradient inequality, robustness, computational analysis.

AMS Subject Classification: 35K57, 35K65, 35B40, 35B41.

1 Introduction

Global Forest Resources Assessment 2020 (FRA 2020)[1] declares that there are 4.06 billion hectares forests around the world, cover nearly 1/3 of land globally. Forests, which are found around the globe, are the largest terrestrial ecosystem of Earth by area, with tropical moist or dry forests around the Equator, temperate forests at the middle latitudes, and boreal forests in subarctic climates. Most importantly, forests provide a diversity of ecosystem services including biodiversity, carbon sequestration, purifying water, aiding in regulating climate [19]. Meanwhile, anthropic activities and forest ecosystems interact with each other. Anthropogenic factors that can affect forests include illegal or unsustainable logging, urban sprawl, human-caused forest fires, acid rain, invasive species, etc [32]. There are also many natural factors that can cause changes in forests over time, including forest fires, pollution, insect pests, diseases, competition between species, as well as the impacts of climate change [22]. However, the impact of these accidental factors on forest ecosystems can not be fully described by non-random forest dynamics. In the past decades, scientists have continued to study global warming and its impact on Earth, and it is a great challenge for the scientific community to better understand the dynamics of forest ecosystems under the impact of global warming. In this paper, our aim is to study, through a mathematical modelling approach relying on differential equations, the dynamics of forest ecosystems associated with several perturbations, which are caused by global warming and anthropic activities.

In [20], an age-structured forest kinematic model determined by a system of parabolic-ordinary differential equations was firstly investigated. The formation of the *ecotone*, which corresponds to the boundary between the forest ecosystem and its neighbor ecosystem, was proved to be faithfully reproduced by the model.

[*]Laboratoire des Sciences du Numérique, LS2N UMR CNRS 6004, Université de Nantes, France. Corresponding author: lu.li@univ-nantes.fr

[†]Laboratoire des Sciences du Numérique, LS2N UMR CNRS 6004, Université de Nantes, France.

[1]https://www.fao.org/forest-resources-assessment/2020/en/

Afterwards, the dynamics of the age-structured forest model has been analyzed by several researchers in a series of papers. The asymptotic behavior of the forest model was notably investigated in [21] (see also Chapter 11 in [38] and the references cited therein). Recently, in [17], it was proved that the trajectories of the model weakly converge to stationary solutions. In [6], an improvement of the model taking into account the water resource was studied. In parallel, a simplified forest model, without any age-structure, was introduced in [2] and [3], where a result of non-existence of the global attractor was established. Here, we consider a forest kinematic model with a perturbation, which can be written as

$$\frac{\partial u}{\partial t} = \alpha w - q(u) - \mu p(u), \qquad \frac{\partial w}{\partial t} = \delta \Delta w - \beta w + \alpha u, \tag{1}$$

where the unknown functions u, w denote the densities of trees and seeds, respectively, in a domain $\Omega \subset \mathbb{R}^2$ modelling a geographical region occupied by a forest. As detailed below, u satisfies a nonlinear ordinary differential equation involving a perturbation $p(u)$ of a given nonlinearity $q(u)$, and w satisfies a reaction-diffusion equation. Very recently, the dynamics of the perturbed forest model (1) was investigated in [4] by geometric methods, in a one dimensional domain, under restrictive symmetry assumptions. However, these geometric methods cannot be extended to a two-dimensional domain, and the symmetry assumption was central in the paper. Therefore, our aim is to continue the analysis of the perturbed forest model (1), by overcoming the space dimension and symmetry restrictions considered in [4].

Main contributions. In the present paper, we consider a general perturbation of the nonlinearity $q(u)$ involved in the first equation of system (1) and study the asymptotic behavior of the degenerate forest kinematic model in 1D and 2D. We establish, without any symmetry assumption, a new result on the convergence of the solutions towards stationary solutions and we prove non trivial statements on the robustness of the flow and of the weak attractors, under the action of the perturbation parameter, in a functional context which is characterized by a lack of compactness. We also improve the asymptotic analysis by applying a computational procedure, based on an original algorithm inspired from the Statistical Model Checking framework [23], to clarify the convergence result. We show that the perturbation succeeds in faithfully reproducing ecological properties of great interest, as highlighted by our numerical results. We emphasize that the first challenge in our research comes from the structure of ODE coupled with PDE, which explains the non-existence of the global attractor of the system; the second challenge follows from the multiple parameters in the generalised perturbation. However, our main results are only valid under a monotonicity assumption similar to that considered in [17]. For the non-monotone case, to the best of our knowledge, there is no such a rigorous result (see [2, 10] for limited results on the unperturbed problem). Finally, we show with a numerical approach that the perturbed forest model exhibits the formation of chaotic patterns, which are of great ecological interest.

We also emphasize that the age-structure forest model presented in [20] and the simplified forest model introduced in [2] present remarkable similarities with degenerate reaction-diffusion systems arising in other domains of life science. Indeed, models very similar to system (1) were studied in [1] or [26] for modelling the dynamics of interacting species with one sedentary species, and in [18] or [25] for studying cellular dynamics in microbiology. Therefore, the methods and results presented in our paper bring a novel knowledge for a large class of systems arising in life science, and not only in forest ecology.

Our paper is organized as follows. In Section 2, we firstly present the forest kinematic model, its well-posedness, and the Lyapunov function governing the dynamical system. We further characterize the ω-limit sets of the global solutions, which consist of equilibria. In Section 3, under suitable convexity assumptions on the parameters, we prove the asymptotic convergence result (Theorem 2) by applying the Łojasiewicz-Simon gradient inequality (Proposition 7). It is remarkable that the conclusion only holds when the potential of the perturbation is convex. Besides, we present a computational analysis (Algorithm 1) of the asymptotic behavior of the system to further clarify the convergence result. In Section 4, we study the long time behavior of the forest model when the perturbation parameter μ tends to 0. We prove the continuity of the flow (Theorem 5), and in the monotone case, we can further prove the continuity of the stationary solutions (Theorem 6), which is nontrivial, and yields the robustness of the weak attractors (Theorem 7). We also analyze the case of a strong perturbation and show how it drives the system to converge to the trivial equilibrium. Finally, in Section 5, we present several numerical simulations, which help better understand how the ecotone can be shifted, and how intermediate ecosystems can emerge under different climatic perturbations. We also show that randomly generated initial conditions can lead to chaotic patterns.

2 Setting of the problem and preliminary results

In this paper, we consider the following initial boundary value problem:

$$\begin{cases} \dfrac{\partial u}{\partial t} = \alpha w - q_\mu(u) & \text{in } (0,+\infty)\times\Omega, \\ \dfrac{\partial w}{\partial t} = \delta\Delta w - \beta w + \alpha u & \text{in } (0,+\infty)\times\Omega, \\ \dfrac{\partial w}{\partial \nu} = 0 & \text{on } (0,+\infty)\times\Gamma, \\ u(0,x) = u_0(x),\ w(0,x) = w_0(x) & \text{in } \Omega, \end{cases} \tag{2}$$

in a bounded and regular domain $\Omega \subset \mathbb{R}^2$ with boundary Γ. The domain Ω models a geographical area occupied by a forest. The unknown functions $u = u(t,x)$ and $w = w(t,x)$ respectively correspond to the densities of the trees and the air-borne seeds. The biological coefficients α, β are the seed production and seed deposition rates; δ is the diffusion rate of seeds in the air; $q_\mu(u)$ denotes the mortality of the trees, which is a smooth function associated with a perturbation term, given as

$$q_\mu(u) = q(u) + \mu p(u), \quad q(u) = u[a(u-b)^2 + c], \quad \mu \geq 0,\ u \in \mathbb{R}, \tag{3}$$

where a, b, c are positive coefficients. We assume that the parameters α, β, δ and μ are positive ($\mu = 0$ leads to unperturbed situation of the system (2)). And the perturbation $p(u)$ is continuously differentiable in $\mathbb{R}$ and satisfies:

$$|p(s)| + |p'(s)| \leq M_1, \quad \forall s \in \mathbb{R},\ M_1 > 0. \tag{4}$$

Note that the function $q_\mu(u)$ derives from a potential $Q_\mu(u)$ written as

$$Q_\mu(u) = \int_0^u (q(\xi) + \mu p(\xi))d\xi, \quad u \in \mathbb{R}. \tag{5}$$

In this paper, we prove a Łojasiewicz-Simon gradient inequality under the assumption:

$$c - \frac{1}{3}ab^2 + \mu p'(u) \geq 0, \tag{6}$$

which implies that the potential $Q_\mu(u)$ given by (5) is convex. Equivalently, we have

$$Q''_\mu(u) = \frac{1}{3}a(3u-2b)^2 + c - \frac{1}{3}ab^2 + \mu p'(u) \geq 0,$$

where $q_0 = \min\limits_{u\in\mathbb{R}} Q''_\mu(u) = c - \frac{1}{3}ab^2 + \mu p'(u) \geq 0$.

Remark 1. *(i) Assumption (6) implies that there exists a positive constant μ_1 such that $q_\mu(u)$ is monotone on $\mathbb{R}$ for all $0 \leq \mu \leq \mu_1$.*
(ii) Note that a special case of perturbation has been studied in [4] by geometric methods, given as

$$q_\mu(u) = q(u) + \mu p(u), \quad q(u) = u(u^2-1), \quad \mu \geq 0,\ u \in \mathbb{R},$$

with symmetry assumption $p(s) + p(-s) = 0$, but the conclusions are only valid in 1D. In this paper, we consider a generalised *perturbation (3) with monotone restriction (6), and study the asymptotic behavior of the perturbed problem (2) in 1D and 2D.*

Throughout this paper, C will stand for positive constants, which may depend on Ω and some other parameters, but are independent of the choice of t, and may change from line to line. Let $\mathcal{C}\big(I,X\big)$ (respectively $\mathcal{C}^1(I,X)$) denote the space of continuous (respectively continuously differentiable) functions defined on an interval $I \subset \mathbb{R}$ with values in a Banach space X. Let $L^p(\Omega)$ and $W^{k,p}(\Omega)$, $p \in [1,\infty]$, $k \in \mathbb{N}$ be the general Lebesgue and Sobolev spaces, equipped with the norms $\|\cdot\|_{L^p}$ and $\|\cdot\|_{W^{k,p}}$, respectively. In particular, for $p = 2$, we simply note $W^{k,2}(\Omega) = H^k(\Omega)$. If V is a Hilbert space with dual V', its inner product is denoted (u,v), $u, v \in V$, and the duality product in $V \times V'$ is denoted $< u, v >$, $u \in V$, $v \in V'$.

2.1 Well-posedness of the forest model

Following [38], we handle the degenerate forest kinetic system (2) in the Banach space X defined by

$$X = L^\infty(\Omega) \times L^2(\Omega),$$

equipped with the product norm $\|U\|_X = \|u\|_{L^\infty} + \|w\|_{L^2}$, for $U = (u, w)^\top \in X$. We will also consider the product space $\mathbb{L}^2(\Omega) = L^2(\Omega) \times L^2(\Omega)$. The space of initial values is given by

$$\mathcal{K} = \left\{U = (u, w)^\top \in X \mid \ u, w \geq 0\right\}.$$

We consider the differential operator Λ defined as the realization of $-\delta\Delta + \beta$ in $L^2(\Omega)$ with the Neumann boundary condition on Γ. It is known that Λ is a positive definite self-adjoint and sectorial operator, of angle strictly less than $\frac{\pi}{2}$, with domain

$$\mathcal{D}(\Lambda) = H^2_N(\Omega) = \left\{w \in H^2(\Omega) \mid \ \frac{\partial w}{\partial \nu} = 0 \text{ on } \Gamma\right\}.$$

Hence, the diagonal operator $A = \operatorname{diag}\{1, \Lambda\}$ is also a sectorial operator in X, with angle strictly less than $\frac{\pi}{2}$, and with domain $\mathcal{D}(A) = L^\infty(\Omega) \times \mathcal{D}(\Lambda)$. Next, we consider an exponent $\eta \in \left(\frac{3}{4}, 1\right)$. The sectorial operator Λ admits a fractional power Λ^η whose domain is given by

$$\mathcal{D}(\Lambda^\eta) = H^{2\eta}_N(\Omega) = \left\{w \in H^{2\eta}(\Omega) \mid \frac{\partial w}{\partial \nu} = 0 \text{ on } \Gamma\right\},$$

where $H^{2\eta}(\Omega)$ is the interpolation space $W^{2\eta,2}(\Omega)$. We have the continuous embeddings

$$H^{2\eta}(\Omega) \subset \mathcal{C}\left(\bar{\Omega}\right) \subset L^\infty(\Omega) \subset L^2(\Omega). \tag{7}$$

Note that the norms $\|u\|_{\mathcal{D}(\Lambda^\eta)}$ and $\|\Lambda^\eta u\|_{L^2(\Omega)}$ are equivalent. The diagonal operator A also admits a fractional power A^η and its domain is given by $\mathcal{D}(A^\eta) = L^\infty(\Omega) \times H^{2\eta}_N(\Omega)$.

In this way, the degenerate forest kinematic system (2) can be written in an abstract form

$$\begin{cases} \dfrac{dU}{dt} + AU = F_\mu(U), \quad t > 0, \\ U(0) = U_0, \end{cases} \tag{8}$$

where $F_\mu(U)$ is the nonlinear operator defined by

$$F_\mu(U) = \begin{pmatrix} \alpha w - q_\mu(u) + u \\ \alpha u \end{pmatrix}, \quad U = (u, w)^\top \in \mathcal{D}(A^\eta).$$

Note that the domain of the nonlinear operator F_μ is uniform with respect to the perturbation parameter μ.

Based on the same techniques applied in Chapter 11 of [38], the dissipative estimate and the existence of global solution of the problem (8) can be established. Here, we omit the proof.

Theorem 1 (Global solutions and continuous dynamical system)**.** *Let $\mu \geq 0$. For all $U_0 \in \mathcal{K}$, the Cauchy problem defined by (8) admits a unique global solution $U_\mu(t, U_0) = (u_\mu, w_\mu)^\top$ defined on $[0, +\infty)$ in the function space*

$$\begin{aligned} &u_\mu \in \mathcal{C}\left([0, +\infty), L^\infty(\Omega)\right) \cap \mathcal{C}^1\left((0, +\infty), L^\infty(\Omega)\right), \\ &w_\mu \in \mathcal{C}\left((0, +\infty), H^2_N(\Omega)\right) \cap \mathcal{C}\left([0, +\infty), L^2(\Omega)\right) \cap \mathcal{C}^1\left((0, +\infty), L^2(\Omega)\right). \end{aligned}$$

Furthermore, the degenerate forest kinematic system (2) determines a continuous dynamical system $S_\mu(t)$ defined in X by

$$S_\mu(t)U_0 = U_\mu(t, U_0), \quad t \geq 0. \tag{9}$$

Remark 2. *Following [4], we emphasize that the domain of A is* not *compactly embedded in X, although the domain of Λ is compactly embedded in $L^2(\Omega)$. This is due to the absence of diffusion term in the first equation, and partly determines the non-existence of a global attractor (see [2]). However, we can not show that the absorbing set $\mathcal{B}_\mu$ generated by the dynamical system $S_\mu(t)$ is compact, hence it turns out that the study of the asymptotic behavior of the dynamical system can not be described by means of the global attractor. In Section 3, we will bypass this lack of compactness by showing the existence of a family of positively invariant regions.*

2.2 Lyapunov function

It is obvious that the potential $Q_\mu(u)$ defined by (5) satisfies $Q_\mu(u) - \alpha uw \geq -C$, for all $u, w \geq 0$, with $C > 0$. Therefore, we can prove that the dynamical system $(S_\mu(t), \mathcal{K}, X)$ determined by (9) admits a Lyapunov function given by

$$\mathscr{L}_\mu(u,w) = \int_\Omega \left[\frac{\delta}{2}|\nabla w|^2 + \frac{\beta}{2}w^2 dx - \alpha uw + Q_\mu(u)\right] dx. \tag{10}$$

The behavior of the forest model (2) is also governed by the potential $H_\mu(u,w)$ defined by

$$H_\mu(u,w) = \frac{\beta}{2}w^2 - \alpha uw + Q_\mu(u), \qquad u, w \in \mathbb{R}.$$

Note that the convexity of $Q_\mu(u)$ does not imply that $H_\mu(u,w)$ is convex. Besides, a symmetric potential $H(u,w)$ has been studied in [2, 4], but only under symmetry assumptions. Since we consider a generalised perturbation $q_\mu(u)$ in this paper, we can not take advantage of the symmetric properties of $H_\mu(u,w)$ to study the asymptotic behavior of the model (2).

Furthermore, the Lyapunov function provides the following additional estimates of time derivative of the global solutions (see Propositions 11.4 and 11.5 in [38]).

Proposition 1. *For any trajectory $S_\mu(t)U_0 = U_\mu(t)$ of the forest kinematic model (2), $U_0 \in \mathcal{K}$, the time derivative of the global solution is bounded in $L^2\big((1,\infty), \mathbb{L}^2\big)$, that is*

$$\int_1^\infty \left\| \frac{dU_\mu}{dt}(t) \right\|^2_{\mathbb{L}^2} < \infty.$$

Proposition 2. *For any trajectory $S_\mu(t)U_0 = U_\mu(t)$ of the forest kinematic model (2), $U_0 \in \mathcal{K}$, the time derivative of the global solution $\frac{dU_\mu}{dt}(t)$ converges to 0 as $t \to \infty$ in the $\mathbb{L}^2$ norm.*

Remark 3. *The convergence of global solutions can be obtained as long as we have $\frac{dU_\mu}{dt}(t) \in L^1\big((1,\infty), \mathbb{L}^2\big)$. However, it can not be directly deduced from the above two propositions. To overcome this difficulty, we prove additional properties of the Lyapunov function and the global solutions, and we also prove the Łojasiewicz-Simon gradient inequality. Then, the addititonal estimation of the time derivative of the global solution can be deduced, so that we can further prove the asymptotic convergence result in Section 3.*

2.3 Constant and non-constant stationary solutions

The forest kinematic model (2) admits constant and non-constant stationary solutions. The constant stationary solutions satisfy

$$\begin{cases} \alpha w - q_\mu(u) = 0, \\ -\beta w + \alpha u = 0. \end{cases} \tag{11}$$

The solutions of the above system correspond to the intersection points between the function $q_\mu(u)$ and the line $\frac{\alpha^2}{\beta}u$. For $\mu = 0$, system (11) admits three homogeneous stationary solutions, which are denoted by $O = (0,0)^\top$, $U^- = (u^-, w^-)^\top$ and $U^+ = (u^+, w^+)^\top$ (with $0 < u^- < u^+$).

It follows from the approach in [21] that the constant stationary solutions $O = (0,0)^\top$, $U^+ = (u^+, w^+)^\top$ are stable, and the constant stationary solution $U^- = (u^-, w^-)^\top$ is unstable. For $\mu > \mu_1$ (where μ_1 is given in Remark 1), the number of constant stationary solutions can be greater than 3. In the sequel, we denote by

$$U_\mu^+ = (u_\mu^+, w_\mu^+)^\top \tag{12}$$

the greatest constant stationary solution of the perturbed system (11). Moreover, we assume that there exists a positive constant $\mu_2 > \mu_1 > 0$, such that, for $\mu > \mu_2$, the trivial solution O is the only constant stationary solution.

Next, the non-constant stationary solutions are determined by the elliptic problem

$$\begin{cases} \alpha\bar{w} - q_\mu(\bar{u}) = 0 & \text{in } \Omega, \\ \delta\Delta\bar{w} - \beta\bar{w} + \alpha\bar{u} = 0 & \text{in } \Omega, \\ \dfrac{\partial\bar{w}}{\partial v} = 0 & \text{on } \Gamma. \end{cases} \tag{13}$$

We will prove that the non-constant stationary solutions describe the asymptotic behavior of the forest kinematic model (2). Indeed, based on the theories in Section 4.2 of Chapter 11 in [38], for each $U_0 \in \mathcal{K}$, we can introduce a modified L^2-ω-limit set of the global solution $U_\mu(t)$ by setting

$$L^2\text{-}\omega_\mu(U_0) = \left\{\bar{U}_\mu \in X; \exists t_n \nearrow \infty \text{ such that } \|U_\mu(t_n) - \bar{U}_\mu\|_{\mathbb{L}^2} \to 0\right\}. \tag{14}$$

Then, adapting the proof of Theorems 11.4 and 11.5 in [38], the following proposition can be established.

Proposition 3. *Let (6) hold, and let $U_0 \in \mathcal{K}$. Then, the L^2-ω-limit set L^2-$\omega_\mu(U_0)$ is nonempty. Furthermore, the set consists of equilibria of (2), i.e., $\bar{U}_\mu = (\bar{u}, \bar{w})^\top$ satisfies (13).*

Our aim in Section 3 is to prove that the global solutions $U_\mu(t) = S_\mu(t)U_0$ converge towards the heterogeneous stationary solution $\bar{U}_\mu$ by applying the Łojasiewicz-Simon gradient inequality (see [17, 24]).

3 Convergence towards stationary solutions

In this section, we establish our main convergence result. In order to simplify the notations, we use $U_\mu(t) = (u, w)^\top$ instead of $U_\mu(t) = (u_\mu, w_\mu)^\top$ to denote the global solution to (2) with the initial value $U_0 \in \mathcal{K}$, and we fix $(\bar{u}, \bar{w})^\top = \bar{U}_\mu \in L^2$-$\omega(U_0)$. It follows from Theorem 1 that

$$\|u(t)\|_{L^\infty} + \|w(t)\|_{H^2} \le R, \quad 1 \le t < \infty, \tag{15}$$

where $R > 0$ depends only on $\|U_0\|_X$. Then, we have the following propositions.

Proposition 4. *Let (15) be satisfied, and $\bar{U} = (\bar{u}, \bar{w})^\top \in L^2$-$\omega(U_0)$. Then, $\|\bar{u}\|_{L^\infty} \le R$ holds. Moreover, $\bar{w} \in H^2_N(\Omega)$ and $\|\bar{w}\|_{H^2} \le R$ hold.*

Proof. $\|\bar{u}\|_{L^\infty} \le R$ follows as a result of the weak*-compactness of the closed unit ball in $L^\infty(\Omega)$. We next prove that $\bar{w}$ is bounded in $H^2_N(\Omega)$. By definition of the L^2-ω-limit set, there exists a sequence $t_n \nearrow \infty$ such that $w(t_n) \to \bar{w}$ in $L^2(\Omega)$. Since $H^2_N(\Omega)$ is sequentially weakly compact and $w(t_n)$ is a bounded sequence in $H^2_N(\Omega)$, there exists a subsequence $w(t'_n)$ such that $w(t'_n)$ has a weak limit $\tilde{w}$ in $H^2_N(\Omega)$. Thus, $w(t'_n) \to \tilde{w}$ in $L^2(\Omega)$, so $\tilde{w} = \bar{w} \in H^2_N(\Omega)$. We further have $\|\bar{w}\|_{H^2} \le \liminf_{t'_n \to \infty} \|w(t'_n)\|_{H^2} \le R$, which completes the proof. □

Proposition 5. *Let (15) be satisfied, and $\bar{U}_\mu = (\bar{u}, \bar{w})^\top \in L^2$-$\omega(U_0)$. Then, there exists a time sequence $t_n \nearrow \infty$ such that $U_\mu(t_n) \to \bar{U}_\mu$ in $L^2(\Omega) \times H^1_N(\Omega)$.*

Proof. It directly follows from the definition of L^2-ω-limit set that there exists a sequence $t_n \nearrow \infty$ such that $U_\mu(t_n) \to \bar{U}_\mu$ in $\mathbb{L}^2$. Moreover, the estimate (15) yields that $\|w(t) + \bar{w}\|_{H^2} \le 2R$ for all $t \ge 1$, we thus apply the interpolation inequality to have $\|w(t_n) - \bar{w}\|_{H^1} \le \|w(t_n) - \bar{w}\|^{\frac{1}{2}}_{H^2} \|w(t_n) - \bar{w}\|^{\frac{1}{2}}_{L^2} \le \sqrt{2R}\|w(t_n) - \bar{w}\|^{\frac{1}{2}}_{L^2} \to 0$ as $t_n \to \infty$. □

We then set $V = L^2(\Omega) \times H^1_N(\Omega)$ in the rest of the paper.

3.1 Modification of the Lyapunov function

In order to consider the Lyapunov function given by (10) on the space V, we need to modify the potential $Q_\mu(u)$ such that $Q_\mu(u) = \mathcal{O}(u^2)$ when $|u| \gg 1$, where $\mathcal{O}(\cdot)$ is big **O** notation, without changing the value $\mathscr{L}_\mu$ on the global solution $U_\mu(t)$ and $\bar{U}_\mu$.

Therefore, we introduce the function $\tilde{Q}_\mu : \mathbb{R} \to \mathbb{R}$ admitting the following properties:
(i) $\tilde{Q}_\mu(u) = Q_\mu(u)$ for $u \in (-1, R+1)$;
(ii) $\tilde{Q}_\mu(u) = \mathcal{O}(u^2)$ for $u \in (-\infty, -1] \cup [R+1, \infty)$;

(iii) $\tilde{Q}_\mu \in \mathcal{C}^2(\mathbb{R})$ and the second derivative satisfies

$$0 < q_0 \le \tilde{Q}''_\mu(u) \le q_1 \quad \text{for any} \quad u \in \mathbb{R}, \tag{16}$$

with some constant $q_1 > 0$ (recall that $q_0 = c - \frac{1}{3}ab^2 + \mu p'(u)$, as defined in (6)).

Based on the modified function $\tilde{Q}_\mu$, we obtain the modified Lyapunov function $\tilde{\mathscr{L}}_\mu : V \to \mathbb{R}$, written as

$$\tilde{\mathscr{L}}_\mu(u,w) = \int_\Omega \left[\frac{\delta}{2}|\nabla w|^2 + \frac{\beta}{2}w^2 - \alpha uw + \tilde{Q}_\mu(u)\right] dx \quad \text{for } U_\mu = (u,w)^\top \in V. \tag{17}$$

Since $\tilde{Q}_\mu(u) = Q_\mu(u)$ for $0 \le u \le R$, we have that $\tilde{\mathscr{L}}_\mu(U_\mu(t)) = \mathscr{L}_\mu(U_\mu(t))$ along the global solution, which implies that $\tilde{\mathscr{L}}_\mu(\cdot)$ plays the same role of a Lyapunov function as $\mathscr{L}_\mu(\cdot)$. Furthermore, the proposition 4 ensures that $\tilde{\mathscr{L}}_\mu(\bar{U}_\mu) = \mathscr{L}_\mu(\bar{U}_\mu)$.

Then, we can prove the above modified Lyapunov function $\tilde{\mathscr{L}}_\mu : V \to \mathbb{R}$ is Fréchet differentiable, and its first Fréchet derivative is denoted as $\tilde{\mathscr{L}}'_\mu : V \to V'$, $V' = L^2(\Omega) \times H^{-1}(\Omega)$. Furthermore, we regard $\Lambda = -\delta\Delta + \beta$ as an isomorphism from $H^1_N(\Omega)$ onto $H^{-1}(\Omega)$.

Proposition 6. *The function $\tilde{\mathscr{L}}_\mu : V \to \mathbb{R}$ is Fréchet differentiable with its derivative*

$$\tilde{\mathscr{L}}'_\mu(U_\mu) = \begin{pmatrix} -\alpha w + q_\mu(u) \\ \Lambda w - \alpha u \end{pmatrix} \in V' \quad \textit{for} \quad U_\mu = (u,w)^\top \in V. \tag{18}$$

In particular, we have $\tilde{\mathscr{L}}'_\mu(\bar{U}_\mu) = 0$ for $\bar{U}_\mu \in L^2\text{-}\omega(U_0)$.

Proof. For $U_\mu = (u,w)^\top, \tilde{U}_\mu = (\tilde{u},\tilde{w})^\top \in V$, we have

$$\begin{aligned} &\tilde{\mathscr{L}}_\mu(U_\mu + \tilde{U}_\mu) - \tilde{\mathscr{L}}_\mu(U_\mu) - \left\langle \begin{pmatrix} -\alpha w + q_\mu(u) \\ \Lambda w - \alpha u \end{pmatrix}, \begin{pmatrix} \tilde{u} \\ \tilde{w} \end{pmatrix} \right\rangle_{V' \times V} \\ &= \int_\Omega [-\alpha \tilde{u}\tilde{w} + \tilde{Q}_\mu(u+\tilde{u}) - \tilde{Q}_\mu(u) - \tilde{Q}'_\mu(u)\tilde{u}]dx + \frac{1}{2}\langle \Lambda\tilde{w}, \tilde{w}\rangle_{H^{-1}\times H^1}. \end{aligned}$$

Due to (16), we have

$$\left| \int_\Omega [\tilde{Q}_\mu(u+\tilde{u}) - \tilde{Q}_\mu(u) - \tilde{Q}'_\mu(u)\tilde{u}]dx \right| \le \frac{q_1}{2}\|\tilde{u}\|^2_{L^2},$$

thus,

$$\left| \tilde{\mathscr{L}}_\mu(U_\mu + \tilde{U}_\mu) - \tilde{\mathscr{L}}_\mu(U_\mu) - \langle \tilde{\mathscr{L}}'_\mu(U_\mu), \tilde{U}_\mu \rangle_{V' \times V} \right| \le C_{\mathscr{L}_\mu}\|\tilde{U}_\mu\|^2_V, \tag{19}$$

where $C_{\mathscr{L}_\mu}$ is positive. The Fréchet derivative (18) is obtained.

Recall that $\bar{U}_\mu \in L^2\text{-}\omega(U_0)$ is a solution of (13). Moreover, since $0 \le \bar{u} \le R$ for a.e. $x \in \Omega$, we know that $\tilde{Q}'_\mu(\bar{u}(x)) = Q'_\mu(\bar{u}(x)) = q_\mu(\bar{u})$. It is obviously to deduce that $\tilde{\mathscr{L}}'_\mu(\bar{U}_\mu) = 0$. □

We note that $\tilde{\mathscr{L}}'_\mu : V \to V'$ is not Fréchet differentiable. Whereas, due to (16), it is easily derived that $\tilde{\mathscr{L}}'_\mu$ is Lipschitz continuous, i.e., there exists a constant $L_0 > 0$ such that

$$\left\|\tilde{\mathscr{L}}'_\mu(U_\mu) - \tilde{\mathscr{L}}'_\mu(\tilde{U}_\mu)\right\|_{V'} \le L_0\|U_\mu - \tilde{U}_\mu\|_V \quad \text{for} \quad U_\mu, \tilde{U}_\mu \in V. \tag{20}$$

3.2 Łojasiewicz-Simon gradient inequality

We then prove that the modified Lyapunov function $\tilde{\mathscr{L}}_\mu(U_\mu)$ give by (17) satisfies the Łojasiewicz-Simon gradient inequality with the following form.

Proposition 7. *Set $\theta \in (0, \frac{1}{2})$. There exists $r > 0$ and $\epsilon > 0$ such that*

$$\left|\tilde{\mathscr{L}}_\mu(U_\mu) - \tilde{\mathscr{L}}_\mu(\bar{U}_\mu)\right| \le \epsilon \left\|\tilde{\mathscr{L}}'_\mu(U_\mu)\right\|^{\frac{1}{1-\theta}}_{V'} \quad \textit{if} \quad \|U_\mu - \bar{U}_\mu\|_V < r. \tag{21}$$

Proof. We divide the proof of the above Łojasiewicz-Simon gradient inequality into three steps.

Step 1. Note that $\Lambda^{-1} : L^2(\Omega) \to L^2(\Omega)$ is a compact self-adjoint operator. Considering the eigenvalue problem

$$\Lambda^{-1} e_n = \eta_n e_n \quad \text{in} \quad L^2(\Omega).$$

As a result of the theory of compact self-adjoint operators, there exists a Hilbert basis $\{e_n\}_{n\in\mathbb{N}} (\subset H^2_N(\Omega))$ of $L^2(\Omega)$ and positive eigenvalues $\{\eta_n\}_{n\in\mathbb{N}}$ such that $\eta_n \searrow 0$ as $n \to +\infty$. For each $N \in \mathbb{N}$, considering orthogonal projection P_N from $L^2(\Omega)$ onto span $\{e_1, \cdots, e_N\}$, then we have the following estimation

$$\|w\|^2_{L^2(\Omega)} \le \|P_N w\|^2_{L^2(\Omega)} + \eta_{N+1} \langle \Lambda w, w\rangle_{H^{-1}\times H^1} \quad \text{for} \quad w \in H^1_N(\Omega).$$

Therefore, for $U_\mu = (u, w)^\top \in V$, the mapping $\mathscr{F} : V \to V'$ is defined as

$$\mathscr{F}(U_\mu) = \tilde{\mathscr{L}}'_\mu(U_\mu) + \begin{pmatrix} 0 \\ \lambda P_N w \end{pmatrix} = \begin{pmatrix} -\alpha w + \tilde{Q}'_\mu(u) \\ \Lambda w - \alpha u + \lambda P_N w \end{pmatrix}, \tag{22}$$

which is a coercive monotone operator if $N \in \mathbb{N}$ and $\lambda > 0$ are sufficiently large. In other words, the following proposition is confirmed.

Proposition 8. *For sufficiently large $N \in \mathbb{N}$ and $\lambda > 0$, there exists a constant $L_1 > 0$ such that*

$$\frac{1}{L_1}\|U_\mu - \tilde{U}_\mu\|^2_V \le \langle \mathscr{F}(U_\mu) - \mathscr{F}(\tilde{U}_\mu), U_\mu - \tilde{U}_\mu\rangle_{V'\times V} \quad \textit{for} \quad U_\mu, \tilde{U}_\mu \in V. \tag{23}$$

Proof. We firstly calculate that

$$\begin{aligned} &\langle \tilde{\mathscr{L}}'_\mu(U_\mu) - \tilde{\mathscr{L}}'_\mu(\tilde{U}_\mu), U_\mu - \tilde{U}_\mu\rangle_{V'\times V} \\ =& -2\alpha \int_\Omega (u-\tilde{u})(w-\tilde{w})dx + \int_\Omega [\tilde{Q}'_\mu(u) - \tilde{Q}'_\mu(\tilde{u})](u-\tilde{u})dx + \langle \Lambda(w-\tilde{w}), w-\tilde{w}\rangle_{H^{-1}\times H^1}. \end{aligned}$$

Due to $\tilde{Q}'_\mu(\xi) - \tilde{Q}'_\mu(\tilde{\xi}) = \int_0^1 \tilde{Q}''_\mu(\theta\xi + (1-\theta)\tilde{\xi})d\theta \times (\xi - \tilde{\xi})$ for $\xi, \tilde{\xi} \in \mathbb{R}$, applying (16) again, we have

$$\int_\Omega [\tilde{Q}'_\mu(u) - \tilde{Q}'_\mu(\tilde{u})](u-\tilde{u})dx \ge q_0 \|u-\tilde{u}\|^2_{L^2},$$

and

$$-2\alpha \int_\Omega (u-\tilde{u})(w-\tilde{w})dx \ge -\tfrac{q_0}{2}\|u-\tilde{u}\|^2_{L^2} - \tfrac{2\alpha^2}{q_0}\|w-\tilde{w}\|^2_{L^2}$$

by employing the Young's inequality. Thus, it follows that

$$\langle \tilde{\mathscr{L}}'_\mu(U_\mu) - \tilde{\mathscr{L}}'_\mu(\tilde{U}_\mu), U_\mu - \tilde{U}_\mu\rangle_{V'\times V} \ge \tfrac{q_0}{2}\|u-\tilde{u}\|^2_{L^2} - \tfrac{2\alpha^2}{q_0}\|w-\tilde{w}\|^2_{L^2} + \langle \Lambda(w-\tilde{w}), w-\tilde{w}\rangle_{H^{-1}\times H},$$

so we have

$$\langle \mathscr{F}(U_\mu) - \mathscr{F}(\tilde{U}_\mu), U_\mu - \tilde{U}_\mu\rangle_{V'\times V} \ge \tfrac{q_0}{2}\|u-\tilde{u}\|^2_{L^2} + (\lambda - \tfrac{2\alpha^2}{q_0})\|w-\tilde{w}\|^2_{L^2} + (1-\lambda\eta_{N+1})\langle \Lambda(w-\tilde{w}), w-\tilde{w}\rangle_{H^{-1}\times H},$$

we finish the proof by choosing $\lambda > \frac{2\alpha^2}{q_0}$ and taking $N \in \mathbb{N}$ large enough (so that η_{N+1} is sufficiently small). □

It follows from Proposition 8 that $\mathscr{F} : V \to V'$ is injective. Furthermore, it is derived by the Browder-Minty theorem (see [34], Theorem 10.49) that $\mathscr{F}$ is surjective. As for its inverse $\mathscr{F}^{-1} : V' \to V$, which is deduced by (23) that

$$\left\|\mathscr{F}^{-1}(U^*_\mu) - \mathscr{F}^{-1}(\tilde{U}^*_\mu)\right\|_V \le L_1 \|U^*_\mu - \tilde{U}^*_\mu\|_{V'} \quad \text{for} \quad U^*_\mu, \tilde{U}^*_\mu \in V'. \tag{24}$$

Step 2. As a restriction of $\mathscr{F}$, consider the mapping $\tilde{\mathscr{F}} : \mathcal{D} \to X$, written as

$$\tilde{\mathscr{F}}(U_\mu) = \begin{pmatrix} -\alpha w + \tilde{Q}'_\mu(u) \\ \Lambda w - \alpha u + \lambda P_N w \end{pmatrix} \in X \quad \text{for} \quad U_\mu = (u, w)^\top \in \mathcal{D}. \tag{25}$$

Then, we obtain the following proposition. Note that the orthogonal projection P_N on $L^2(\Omega)$ is regarded as a bounded linear operator from $H^2_N(\Omega)$ to $L^2(\Omega)$.

Proposition 9. *$\tilde{\mathscr{F}} : \mathcal{U}(\bar{U}_\mu) \subset \mathcal{D} \to X$ is an analytic function, where $\mathcal{U}(\bar{U}_\mu)$ is a neighborhood of $\bar{U}_\mu$ in $\mathcal{D}$.*

Proof. It is easy to prove that mapping $\tilde{Q}'_\mu : L^\infty(\Omega) \to L^\infty(\Omega)$ is analytic at $\bar{u} \in L^\infty(\Omega)$. In fact, if $\tilde{Q}'_\mu$ is analytic at $\bar{u} \in L^\infty(\Omega)$, a neighborhood of $\bar{u}$ exists such that $\tilde{Q}'_\mu$ is analytic on its neighborhood. We omit the proof here. □

In particular, for $U_\mu = (u, w)^\top \in \mathcal{U}(\bar{U}_\mu)$, its first derivative $\tilde{\mathscr{F}}' : \mathcal{U}(\bar{U}_\mu) \to \mathcal{L}(\mathcal{D}, X)$ is given by

$$\tilde{\mathscr{F}}'(U_\mu) = \begin{pmatrix} \tilde{Q}''_\mu(u) & -\alpha \\ -\alpha & \Lambda + \lambda P_N \end{pmatrix} \in \mathcal{L}(\mathcal{D}, X),$$

where the inverse mapping theorem theorem (see [39], Corollary 4.37) is applied. We further have the following proposition.

Proposition 10. *$\tilde{\mathscr{F}}'(\bar{U}_\mu) : \mathcal{D} \to X$ is bijective.*

Proof. Note that the operator T, given by

$$T = \begin{pmatrix} \tilde{Q}''_\mu(u) & -\alpha \\ -\alpha & \Lambda + \lambda P_N \end{pmatrix},$$

belongs to $\mathcal{L}(V, V')$. By using the same approach in the proof of Proposition 8, $\frac{1}{L_1}\|U_\mu\|_V^2 \le \langle TU_\mu, U_\mu\rangle_{V'\times V}$ for $U_\mu \in V$ is obtained. Thus,

$$T \text{ is a linear isomorphism from } V \text{ onto } V'. \tag{26}$$

Let $U^*_\mu = (u^*, w^*)^\top \in X$. Since also $(u^*, w^*)^\top \in V'$, it follows from (26) that there exists a unique $U_\mu = (u, w)^\top \in V$ such that

$$T\begin{pmatrix} u \\ w \end{pmatrix} = \begin{pmatrix} u\tilde{Q}''_\mu(u) - \alpha w \\ -\alpha u + \Lambda w + \lambda P_N w \end{pmatrix} = \begin{pmatrix} u^* \\ w^* \end{pmatrix}$$

It is obviously that $\Lambda w = w^* + \alpha u - \lambda P_N w \in L^2(\Omega)$, and $u = \frac{1}{\tilde{Q}''_\mu(u)}(u^* + \alpha w) \in L^\infty(\Omega)$ by employing (16). Therefore, $\tilde{\mathscr{F}}'(\bar{U}_\mu)$ is bijective from $\mathcal{D}$ to X. □

Due to Proposition 9, Proposition 10 and [39] Corollary 4.37, there exists a neighborhood $\mathcal{V}(\tilde{\mathscr{F}}(\bar{U}_\mu)) \subset X$, such that

$$\tilde{\mathscr{F}} : \mathcal{U}(\bar{U}_\mu) \to \mathcal{V}(\tilde{\mathscr{F}}(\bar{U}_\mu)) \text{ is an analytic diffeomorphism} \tag{27}$$

by choosing sufficiently small $\mathcal{U}(\bar{U}_\mu)$.

Step 3. Considering the finite-dimensional linear space

$$E_N = 0 \times span\{e_1, \cdots, e_N\} \subset \mathcal{D},$$

equipped with the norm $\|\cdot\|_{E_N}$, we then have the norm equivalence

$$\left\|(0, w_N)^\top\right\|_{E_N} = \|w_N\|_{H^1} \quad \text{for} \quad (0, w_N)^\top \in E_N. \tag{28}$$

Therefore, we have the following proposition.

Proposition 11. *There exist constants $\epsilon_0 > 0$ and $r_0 > 0$ such that*

$$\left|\tilde{\mathscr{L}}_\mu \circ \tilde{\mathscr{F}}^{-1}((0, \lambda P_N w)^\top) - \tilde{\mathscr{L}}_\mu(\bar{U}_\mu)\right|^{1-\theta} \le \epsilon_0 \left\|(\tilde{\mathscr{L}}_\mu \circ \tilde{\mathscr{F}}^{-1})'((0, \lambda P_N w)^\top)\right\|_{E'_N} \quad \textit{for} \quad \|w - \bar{w}\|_{H^1} < r_0. \tag{29}$$

Proof. It is obvious that $\tilde{\mathscr{L}}_\mu$ is analytic as a function from $\mathcal{U}(\bar{U}_\mu) \subset \mathcal{D}$ to $\mathbb{R}$. Combined with (27), we have the function composition:

$$\tilde{\mathscr{L}}_\mu \circ \tilde{\mathscr{F}}^{-1} : \mathcal{V}(\tilde{\mathscr{F}}(\bar{U}_\mu)) \cap E_N \to \mathbb{R} \text{ is an analytic function from } E_N \text{ to } \mathbb{R}. \tag{30}$$

Then, employing the classical Łojasiewicz Theorem (see [24]) to assume that $\theta \in (0, \frac{1}{2}]$ and $\epsilon_0, r_1 > 0$ exist, such that

$$\left|\tilde{\mathscr{L}}_\mu \circ \tilde{\mathscr{F}}^{-1}((0,w_N)^\top) - \tilde{\mathscr{L}}_\mu \circ \tilde{\mathscr{F}}^{-1}(\tilde{\mathscr{F}}(\bar{U}_\mu))\right|^{1-\theta} \leq \epsilon_0 \left\|(\tilde{\mathscr{L}}_\mu \circ \tilde{\mathscr{F}}^{-1})'((0,w_N)^\top) - (\tilde{\mathscr{L}}_\mu \circ \tilde{\mathscr{F}}^{-1})'(\tilde{\mathscr{F}}(\bar{U}_\mu))\right\|_{E_N'},$$

if $(0,w_N)\top \in E_N$ satisfies $\|(0, w_N - \lambda P_N \bar{w})^\top\|_{E_N} < r_1$. Note that, it follows from $\tilde{\mathscr{L}}_\mu'(\bar{U}_\mu) = 0$ that $(\tilde{\mathscr{L}}_\mu \circ \tilde{\mathscr{F}}^{-1})'(\tilde{\mathscr{F}}(\bar{U}_\mu)) = \tilde{\mathscr{L}}_\mu'(\tilde{\mathscr{F}}^{-1}(\tilde{\mathscr{F}}(\bar{U}_\mu))) \circ (\tilde{\mathscr{F}}^{-1})'(\tilde{\mathscr{F}}(\bar{U}_\mu)) = \tilde{\mathscr{L}}_\mu'(\bar{U}_\mu) \circ (\tilde{\mathscr{F}}^{-1})'(\tilde{\mathscr{F}}(\bar{U}_\mu)) = 0$. Then we have

$$\left|\tilde{\mathscr{L}}_\mu \circ \tilde{\mathscr{F}}^{-1}((0,w_N)^\top) - \tilde{\mathscr{L}}_\mu(\bar{U}_\mu)\right|^{1-\theta} \leq \epsilon_0 \left\|(\tilde{\mathscr{L}}_\mu \circ \tilde{\mathscr{F}}^{-1})'((0,w_N)^\top)\right\|_{E_N'} \quad \text{if} \quad \|(0, w_N - \lambda P_N \bar{w})^\top\|_{E_N} < r_1. \tag{31}$$

Due to (28), there exists $r_0 > 0$ small enough so that $\|w - \bar{w}\|_{H^1} < r_0$ and $\|(0, w_N - \lambda P_N \bar{w})^\top\|_{E_N} < r_1$. Therefore, (29) can be deduced by (31), we finish the proof of Proposition 11. □

Furthermore, we estimate the right side of (29) to have

$$\begin{aligned}\left\|(\tilde{\mathscr{L}}_\mu \circ \tilde{\mathscr{F}}^{-1})'((0,\lambda P_N w)^\top)\right\|_{E_N'} &= \left\|\tilde{\mathscr{L}}_\mu'(\tilde{\mathscr{F}}^{-1}((0,\lambda P_N w)^\top)) \circ (\tilde{\mathscr{F}}^{-1})'((0,\lambda P_N w)^\top)\right\|_{E_N'} \\ &\leq C_r \left\|\tilde{\mathscr{L}}_\mu'(\tilde{\mathscr{F}}^{-1}((0,\lambda P_N w)^\top))\right\|_{V'},\end{aligned}$$

where the constant C_r is positive and depends only on r_0, we note that it follows from (27) that

$$\left\|(\tilde{\mathscr{F}}^{-1})'((0,\lambda P_N w)^\top)\right\|_{\mathcal{L}(E_N,V)} \leq C_r \quad \text{if} \quad \|w - \bar{w}\|_{H^1} < r_0.$$

For arbitrarily $u \in L^2(\Omega)$, we have

$$\begin{aligned}\left\|\tilde{\mathscr{L}}_\mu'(\tilde{\mathscr{F}}^{-1}((0,\lambda P_N w)^\top))\right\|_{V'} &\leq \left\|\tilde{\mathscr{L}}_\mu'(\tilde{\mathscr{F}}^{-1}((0,\lambda P_N w)^\top)) - \tilde{\mathscr{L}}_\mu'((u,w)^\top)\right\|_{V'} + \left\|\tilde{\mathscr{L}}_\mu'((u,w)^\top)\right\|_{V'} \\ &\leq L_0 \left\|\tilde{\mathscr{F}}^{-1}((0,\lambda P_N w)^\top) - \tilde{\mathscr{F}}^{-1}(\tilde{\mathscr{F}}((u,w)^\top))\right\|_V + \left\|\tilde{\mathscr{L}}_\mu'(U_\mu)\right\|_{V'} \\ &\leq (L_0 L_1 + 1) \left\|\tilde{\mathscr{L}}_\mu'(U_\mu)\right\|_{V'}\end{aligned}$$

by employing (20), (22) and (24). Then, for $U_\mu = (u,w)^\top \in V, \|w - \bar{w}\|_{H^1} < r_0$, it follows that

$$\left|\tilde{\mathscr{L}}_\mu \circ \tilde{\mathscr{F}}^{-1}((0,\lambda P_N w)^\top) - \tilde{\mathscr{L}}_\mu(\bar{U}_\mu)\right|^{1-\theta} \leq \epsilon_0 C_r (L_0 L_1 + 1) \left\|\tilde{\mathscr{L}}_\mu'(U_\mu)\right\|_{V'}. \tag{32}$$

Besides, note that $\tilde{U}_\mu = \tilde{\mathscr{F}}^{-1}((0,\lambda P_N w)^\top) - U_\mu$, it follows from (19) that

$$\begin{aligned}&\left|\tilde{\mathscr{L}}_\mu(U_\mu) - \tilde{\mathscr{L}}_\mu \circ \tilde{\mathscr{F}}^{-1}((0,\lambda P_N w)^\top)\right| \\ =&\left|\tilde{\mathscr{L}}_\mu(U_\mu) - \tilde{\mathscr{L}}_\mu(U_\mu + \tilde{U}_\mu)\right| \\ \leq&\left\|\tilde{\mathscr{L}}_\mu'(U_\mu)\right\|_{V'} \left\|\tilde{\mathscr{F}}^{-1}((0,\lambda P_N w)^\top) - U_\mu\right\|_V + C_{\mathscr{L}_\mu} \left\|\tilde{\mathscr{F}}^{-1}((0,\lambda P_N w)^\top) - U_\mu\right\|_V^2 \\ \leq&(L_1 + C_{\mathscr{L}_\mu} L_1^2) \left\|\tilde{\mathscr{L}}_\mu'(U_\mu)\right\|_{V'}^2,\end{aligned} \tag{33}$$

again, (22) and (24) are applied. Therefore, it is derived from (32) and (33) that

$$\begin{aligned}\left|\tilde{\mathscr{L}}_\mu(U_\mu) - \tilde{\mathscr{L}}_\mu(\bar{U}_\mu)\right| &\leq \epsilon_0 C_r (L_0 L_1 + 1) \left\|\tilde{\mathscr{L}}_\mu'(U_\mu)\right\|_{V'}^{\frac{1}{1-\theta}} + (L_1 + C_{\mathscr{L}_\mu} L_1^2) \left\|\tilde{\mathscr{L}}_\mu'(U_\mu)\right\|_{V'}^2 \\ &\leq C_0 \left\|\tilde{\mathscr{L}}_\mu'(U_\mu)\right\|_{V'}^{\frac{1}{1-\theta}} \quad \text{if} \quad \|U_\mu - \bar{U}_\mu\|_V < r,\end{aligned}$$

where the constant C_0 is positive and depends on $\epsilon_0, C_{\mathscr{L}_\mu}, C_r, L_0, L_1$ and θ, by taking $r \in (0, r_0)$ small enough to make sure that $\left\|\tilde{\mathscr{L}}_\mu'(U_\mu)\right\|_{V'}^2 \leq \left\|\tilde{\mathscr{L}}_\mu'(U_\mu)\right\|_{V'}^{\frac{1}{1-\theta}}$. We eventually finish the proof of Proposition 7. □

Remark 4. *Note that the convexity condition (6) is a restrictive one, otherwise (especially, when the perturbation μ is large), the approach we apply in this section can not ensure the Łojasiewicz-Simon gradient inequality still holds. Therefore, we can not further prove the following asymptotic convergence result.*

3.3 Asymptotic convergence result

To prove the asymptotic convergence of global solutions, we firstly present the following lemma (see Appendix in [17] and Lemma 7.1 in [12] for the proof), which gives a sufficient condition in order that a function in $L^2(0,\infty)$ is also in $L^1(0,\infty)$.

Lemma 1. *Let $F:(0,\infty)\to[0,\infty)$ be a nonnegative continuous function satisfying $F\in L^2(0,\infty)$. Assume that an interval $I=(T,T')\subset(0,\infty)$, an exponent $\alpha\in(1,2)$, and a constant $\kappa>0$ exist such that*

$$\left(\int_t^\infty F(\tau)^2 d\tau\right)^\alpha \le \kappa F(t)^2,\ \forall t\in I. \tag{34}$$

Then, the following inequality holds:

$$\int_I F(\tau)d\tau \le \kappa' \|F\|^{\alpha'}_{L^2(T,\infty)}, \tag{35}$$

where $\alpha'>0$ depends only on α, and $\kappa'>0$ depends only on α and κ.

Then, we have the following proposition.

Proposition 12. *For sufficiently large time $T>0$, There exists a constant $\kappa>0$. If $\|U_\mu(t)-\bar U_\mu\|_V<r$, $t>T$, then*

$$\left(\int_t^\infty \left\|\frac{dU_\mu}{d\tau}(\tau)\right\|^2_{\mathbb{L}^2} d\tau\right)^{2(1-\theta)} \le \kappa \left\|\frac{dU_\mu}{dt}(t)\right\|^2_{\mathbb{L}^2}. \tag{36}$$

Proof. Since we have $\left\|\frac{dU_\mu}{dt}(t)\right\|_{\mathbb{L}^2}\to 0$ as $t\to\infty$ due to Proposition 2, take $T>1$ large enough such that

$$\left\|\frac{\partial u}{\partial t}(t)\right\|_{L^2}<1,\ \forall t>T,$$

and we fix such time $T>1$. Due to the definition of L^2-$\omega(U_0)$, there exists a $t\in(T,\infty)$ such that $\|U_\mu(t)-\bar U_\mu\|_V<r$.

Next, we have

$$-\int_\Omega\left(\left|\frac{\partial u}{\partial t}\right|^2+\left|\frac{\partial w}{\partial t}\right|^2\right)dx=\frac{d}{dt}\int_\Omega\left[\frac{\delta}{2}|\nabla w|^2dx+\frac{\beta}{2}w^2dx-\alpha uw+Q_\mu(u)\right]dx.$$

By integrating the above equation with respect to time on (t,∞), we have

$$\int_t^\infty\int_\Omega\left(\left|\frac{\partial u}{\partial\tau}(\tau)\right|^2+\left|\frac{\partial u}{\partial\tau}(\tau)\right|^2\right)dxd\tau=\tilde{\mathscr{L}}_\mu(U_\mu(t))-\tilde{\mathscr{L}}_\mu(\bar U_\mu),$$

it is deduced from (21) that

$$\int_t^\infty\left(\left\|\frac{\partial u}{\partial\tau}(\tau)\right\|^2_{L^2}+\left\|\frac{\partial w}{\partial\tau}(\tau)\right\|^2_{L^2}\right)d\tau\le\epsilon\|\tilde{\mathscr{L}}'_\mu(U_\mu(t))\|^{\frac{1}{1-\theta}}_{V'}. \tag{37}$$

Then, it follows from Proposition 6 that $\tilde{\mathscr{L}}'_\mu(U_\mu(t))=(-\frac{\partial u}{\partial t},-\frac{\partial w}{\partial t})^\top\in V'$, which yields

$$\|\tilde{\mathscr{L}}'_\mu(U_\mu(t))\|^2_{V'}\le C\left(\left\|\frac{\partial u}{\partial t}(t)\right\|^2_{L^2}+\left\|\frac{\partial w}{\partial t}(t)\right\|^2_{H^{-1}}\right).$$

Combined with (37), we have

$$\int_t^\infty\left\|\frac{dU_\mu}{d\tau}(\tau)\right\|^2_{\mathbb{L}^2}d\tau\le C'\left\|\frac{dU_\mu}{dt}(t)\right\|^{\frac{1}{1-\theta}}_{\mathbb{L}^2},$$

where, C' depends on positive constants ϵ and $\theta\in(0,\frac12)$. We finish the proof. □

Furthermore, we prove the following lemma.

Lemma 2. *There exists a sufficiently large $t_N > 0$ such that $\|U_\mu(t) - \bar{U}_\mu\|_V < r$ for all $t \geq t_N$.*

Proof. Owing to Proposition 5, there exists a time sequence $t_n \nearrow \infty$ such that $U_\mu(t_n) \to \bar{U}_\mu$ in V. Thus, a sufficiently large N_0 exists to ensure that

$$\|U_\mu(t_n) - \bar{U}_\mu\|_V \leq \frac{r}{3}, \ \forall n \geq N_0.$$

Moreover, for $n \geq N_0$, set $t_n' = \inf\{t \in (t_n, \infty); \ \|U_\mu(t) - \bar{U}_\mu\|_V = r\}$; in particular, $t_n' = \infty$ when $\|U_\mu(t) - \bar{U}_\mu\|_V < r$ for all $t \geq t_n$. Recalling Lemma 1, we take $F(t) = \left\|\frac{dU_\mu}{dt}(t)\right\|_{\mathbb{L}^2}$, $\alpha = 2(1-\theta)$, $T = t_n$, and $T' = t_n'$. Then, due to Proposition 12, we have

$$\int_{t_n}^{t_n'} \left\|\frac{dU_\mu}{d\tau}(\tau)\right\|_{\mathbb{L}^2} d\tau < \kappa' \left(\int_{t_n}^{\infty} \left\|\frac{dU_\mu}{dt}(t)\right\|_{\mathbb{L}^2}^2 dt\right)^{\frac{\theta'}{2}},$$

where θ' depends only on θ. Therefore,

$$\|U_\mu(t_n') - U_\mu(t_n)\|_V \leq C \int_{t_n}^{t_n'} \left\|\frac{dU_\mu}{d\tau}(\tau)\right\|_{\mathbb{L}^2} d\tau \leq C\kappa' \left(\int_{t_n}^{\infty} \left\|\frac{dU_\mu}{dt}(t)\right\|_{\mathbb{L}^2}^2 dt\right)^{\frac{\theta'}{2}}.$$

Then, $\|U_\mu(t_N') - U_\mu(t_N)\|_V \leq \frac{r}{3}$ can be derived by taking $N \geq N_0$ large enough. Besides, we know that $t_N' = \infty$, for such $N \geq N_0$. Indeed, suppose that $t_N' < \infty$. Then, $\|U_\mu(t_N') - \bar{U}_\mu\|_V = r$. On the other hand, we have

$$\|U_\mu(t_N') - \bar{U}_\mu\|_V \leq \|U_\mu(t_N') - U_\mu(t_N)\|_V + \|U_\mu(t_N) - \bar{U}_\mu\|_V \leq \frac{2r}{3},$$

which completes the proof. □

Finally, we conclude the asymptotic convergence result.

Theorem 2. *Assume that assumption (6) holds. Let $U_\mu(t) = S_\mu(t)U_0$ be the global solution to the forest kinematic model (2) with initial value $U_0 \in \mathcal{K}$, and let $\bar{U}_\mu \in L^2$-$\omega(U_0)$ be a stationary solution to (2). Then, we have $U_\mu(t) \to \bar{U}_\mu$ in $\mathbb{L}^2(\Omega)$ as $t \to \infty$.*

Proof. Due to Lemma 1, 2 and Proposition 12, there exists a sufficiently large $t_N > 0$ such that

$$\int_t^{\infty} \left\|\frac{dU_\mu}{d\tau}(\tau)\right\|_{\mathbb{L}^2} d\tau \leq \kappa' \left(\int_t^{\infty} \left\|\frac{dU_\mu}{d\tau}(\tau)\right\|_{\mathbb{L}^2}^2 d\tau\right)^{\frac{\theta'}{2}}, \ \forall t \geq t_N.$$

Furthermore, since the definition of L^2-$\omega(U_0)$, there exists a time sequence $t_n \nearrow \infty$ such that $U_\mu(t_n) \to \bar{U}_\mu$ in $\mathbb{L}^2(\Omega)$. Then, we have

$$\begin{aligned}\|U_\mu(t) - \bar{U}_\mu\|_{\mathbb{L}^2} &\leq \|U_\mu(t) - U_\mu(t_n)\|_{\mathbb{L}^2} + \|U_\mu(t_n) - \bar{U}_\mu\|_{\mathbb{L}^2} \\ &\leq \int_t^{t_n} \left\|\frac{dU_\mu}{d\tau}(\tau)\right\|_{\mathbb{L}^2} d\tau + \|U_\mu(t_n) - \bar{U}_\mu\|_{\mathbb{L}^2},\end{aligned}$$

and when t_n goes to infinity, we obtain

$$\|U_\mu(t) - \bar{U}_\mu\|_{\mathbb{L}^2} \leq \kappa' \left(\int_t^{\infty} \left\|\frac{dU_\mu}{d\tau}(\tau)\right\|_{\mathbb{L}^2}^2 d\tau\right)^{\frac{\theta'}{2}}.$$

Therefore, we conclude the assertion. □

3.4 Computational analysis of the asymptotic behavior

The convergence result established in Theorem 2 guarantees that the global solutions of system (2) necessarily converge towards a stationary solution. However, it does not distinguish the convergence towards a *constant* stationary solution (which is a solution of system (11)) or towards a *non-constant* stationary solution (which is a solution of system (13)). Therefore, it is of great interest to better analyze the convergence towards *non-constant* stationary solutions, since they correspond to the formation of the ecotone, which is the ecological transition between the forest and its neighbor ecosystem. In this section, since it is known that the complete asymptotic analysis of system (2) by theoretical methods is very delicate (see notably [21] and [2]), we perform a computational analysis of the asymptotic behavior of system (2). Our computational method is adapted from the Statistical Model Checking method [23], which was very recently applied in [5] to the study of the forest model perturbed by a discrete probabilistic process. This method relies on Monte-Carlo techniques and provides formal guarantees that can be expressed by means of confidence intervals.

We now describe our computational approach. We first fix a number of time steps $T \gg 1$. We denote by Φ_T the set of global solutions of system (2) in the functional space X, which converge to a non-constant stationary solution. Next, we consider randomly generated initial conditions $U_0 = (u_0, w_0)^\top$ satisfying

$$\frac{1}{10}u^- \leq u_0(x) \leq \frac{19}{10}u^-, \qquad \frac{1}{10}w^- \leq w_0(x) \leq \frac{19}{10}w^-, \qquad x \in \Omega. \tag{38}$$

The latter conditions are chosen in order to obtain a distribution of $U_0 = (u_0, w_0)^\top$ in a neighborhood of the saddle equilibrium $U^- = (u^-, w^-)^\top$, while guaranteeing non-negativity. Our aim is to estimate the probability for a global solution $U(t, U_0)$, starting from an initial condition of the form (38), to belong to the set Φ_T. Hence, we fix a precision factor $\varepsilon > 0$ and an error rate $\vartheta \in (0, 1)$. In order to perform the estimation using the Monte-Carlo method, we sample a fixed amount $(U_i)_{1 \leq i \leq N}$ of global solutions of system (2). Each global solution U_i is associated with a Bernoulli variable X_i regarding the satisfaction of Φ_T, that is, $X_i = 1$ if and only if $U_i \in \Phi_T$. Using Theorem 1 in [16], we obtain the following estimation, provided $N \geq 4 \log\left(\frac{2}{\vartheta}\right)/\varepsilon^2$:

$$\mathbb{P}\left(\left|\mathbb{P}(\Phi_T) - \frac{1}{N}\sum_{1 \leq i \leq N} X_i\right| \leq \varepsilon\right) \geq 1 - \vartheta. \tag{39}$$

In the following, we will fix $T = 1000$ and $\varepsilon = \vartheta = 0.1$, which will therefore require $N \geq 1200$ samples of system (2). With these notations, we consider Algorithm 1 below. In this algorithm, we generate randomly an initial condition U_0 in line 7. In line 8, we compute an approximation $\tilde{U}(t, U_0)$ of the global solution $U(t, U_0)$ of system (2). This numerical approximation is performed by applying a splitting numerical scheme of Strang type [36], with a classical Runge-Kutta method in time and a finite elements discretization in space. The discretization in space of the domain Ω requires to introduce a mesh domain Ω_{mesh} (lines 9, 10). We emphasize that this splitting scheme is convergent, which guarantees that the probability for a global solution $U(t, U_0)$ to belong to the set Φ_T can be estimated by the probability for its numerical approximation $\tilde{U}(t, U_0)$ to belong to the set Φ_T. In lines 9, 10, 11, we detect a non-constant equilibrium by counting the numbers of points $x \in \Omega_{mesh}$ such that $u(T, x)$ is greater or less than u^-, with a numerical margin m. In practice, Algorithm 1 was implemented with the FreeFem++ language [15], and ran on the computation server of the Laboratory of Digital Sciences in Nantes (France), in a GNU/Linux environment, with a total execution of about 8 days. The complete code is available on the public repository

https://gitlab.univ-nantes.fr/forest/computational-analysis-of-the-forest-model,

along with the complete results of its execution.

The execution of Algorithm 1 leads to the following Computer Assisted Theorem.

Theorem 3 (Computer assisted analysis of the asymptotic behavior)**.** *Assume that $\alpha = 1$, $\beta = 1$, $a = 0.6$, $b = 1$, $c = 0.9$, $\delta = 10$ and $\mu = 0$. Assume morevover that Ω is an elliptic domain of dimensions $L = 50$ and $\ell = 30$. Then, the probability for a global solution $U(t, U_0)$ of system (2), starting from an initial condition U_0 satisfying (38), to converge towards a non-constant stationary solution satisfies the following numerical estimate:*

$$\mathbb{P}(\Phi_T) \gtrsim 0.479.$$

Obviously, Algorithm 1 can be applied to other parameter values, provided assumption (6) is satisfied. We show in Table 1 some results of the execution of Algorithm 1. A non-constant stationary is detected

Algorithm 1 Computational analysis of the asymptotic behavior of system (2)

variables
  integer $N \leftarrow 1200$; // Number of simulations, guaranteeing (39)
  integer i;
  integers $n_0 \leftarrow 0$, n_1, n_2; // Counters for analyzing the asymptotic behavior
  real $m \leftarrow 0.1$; // Margin around the saddle u^-
for i from 1 to N **do** // Main loop of the Monte-Carlo algorithm
  generate randomly an initial condition U_0 satisfying (38);
  compute the approximated trajectory $\tilde{U}(t, U_0)$ on $[0, T]$; // (the numerical scheme is convergent)
  $n_1 \leftarrow$ number of points x in Ω_{mesh} such that $u(T, x) > u^- + m$;
  $n_2 \leftarrow$ number of points x in Ω_{mesh} such that $u(T, x) < u^- - m$;
  if $n_1 > 0$ and $n_2 > 0$ **then** // We detect a non-constant equilibrium
    $n_0 \leftarrow n_0 + 1$;
  end if
end for
return n_0/N; // We return the frequency of non-constant equilibria

when the counters n_1 and n_2 are both positive. If one of these counters is equal to zero, then it means that the solution converges towards a constant stationary solution. Overall, an amount of 575 non-constant equilibria were detected, over 1200 simulations, which means that at least 0.479% of the global solutions of system (2) converge to a heterogeneous steady state. Note that the numerical margin m introduced in Algorithm 1 leads to an over approximation of the probability to be estimated, but prevents from low level numerical unexpected behavior. We emphasize that in the sequel, we will obtain additional information on the asymptotic behavior of system (2). Indeed, we will prove the continuity of the flow under a variation of the perturbation parameter μ (see Theorems 5 and 6), which will ensure that the global solutions of system (2) with parameter values close to those given in Theorem 3 converge to non-constant equilibria with a close probability (see Remark 6 below).

Table 1: Partial results of the computational analysis of system (2) with Algorithm 1. Non-constant stationary solutions are detected when $n_1 > 0$ and $n_2 > 0$.

Simulation	1	2	3	4	5	6	7	8	9	10	...	1200
n_1	356	0	137	195	390	230	96	154	0	0	...	0
n_2	236	24	30	140	286	213	383	490	771	170	...	451
n_0	1	1	2	3	4	6	6	7	7	7	...	**575**

4 Robustness of the weak attractors

In this section, we analyze the robustness of the dynamical system (9) determined by the degenerate forest kinetic system (2). As explained previously in Remark 2, we have to face a lack of compactness, which is due to the absence of diffusion in the first equation of system (2). Therefore, as shown in [2], the long time behavior of the dynamical system (9) cannot be described by means of the global attractor. However, following [38], we can still analyze the weak convergence of its orbits in the topology of the Banach space Y, for simplicity, given by

$$Y = \mathbb{L}^2(\Omega) = L^2(\Omega) \times L^2(\Omega). \tag{40}$$

Hence, for $U_0 \in \mathcal{K}$ and $B \subset X$, we consider the weak L^2-ω-limit sets of the dynamical system $S_\mu(t)$ given by

$$\omega_Y^\mu(U_0) = \bigcap_{t \geq 0} \overline{\{S_\mu(s)U_0; t \leq s < \infty\}}^Y, \tag{41}$$

where the closures are in Y. Note that $\omega_\mu^Y(U_0)$ actually coincides with the set L^2-$\omega_\mu(U_0)$ defined in (14).

We bypass the lack of compactness by proving the existence of a family $\{\mathscr{R}_\mu\}$ of positively invariant regions, from which we deduce the continuity of the flow induced by the dynamical system (9). Combined

with the asymptotic convergence result obtained in Section 3.3, we can further prove the continuity of the stationary solutions. Therefore, the robustness of the weak ω-limit sets under the effect of the perturbation parameter μ can be derived. In the end of this section, we address that the case of a small perturbation $\mu \in (0, \mu_1)$ proves to be the most interesting, since the case of a strong perturbation $\mu > \mu_2$ ($\mu_2 > \mu_1 > 0$) leads to trivial dynamics.

4.1 Positively invariant regions

The following theorem establishes the existence of a family of positively invariant regions for the dynamical system $\{S_\mu(t)\}$ defined by (9).

Theorem 4 (Positively invariant region)**.** *Let $\mu \geq 0$. Then the region $\mathscr{R}_\mu \subset X$ defined by*

$$\mathscr{R}_\mu = \Big\{(u, w) \in X \mid (u(x), w(x)) \in R_\mu,\ \forall x \in \mathbb{R}\Big\} \tag{42}$$

with $R_\mu = [0, u_\mu^+] \times [0, w_\mu^+]$ (where (u_μ^+, w_μ^+) is given by (12)) is positively invariant by the flow induced by the degenerate forest kinetic system (2), that is, if $U_0 \in \mathscr{R}_\mu$, then $S_\mu(t)U_0 \in \mathscr{R}_\mu$ for all $t > 0$.

Proof. Let $U_0 \in \mathscr{R}_\mu$, for $t \geq 0$, we denote by $U_\mu(t) = S_\mu(t)U_0$ the global solution of the degenerate reaction-diffusion system (2) stemming from U_0.

We consider a cut-off function χ defined on $\mathbb{R}$ by

$$\chi(s) = \begin{cases} \frac{1}{2}s^2 & \text{if } s < 0, \\ 0 & \text{if } s \geq 0. \end{cases}$$

We observe that χ is continuously differentiable on $\mathbb{R}$, and elementary computations show that the following properties hold for all $r, s \in \mathbb{R}$:

$$\chi(s) \geq 0, \quad \chi'(s) \leq 0, \tag{43}$$

$$0 \leq s\chi'(s) \leq 2\chi(s), \tag{44}$$

$$r\chi'(s) + s\chi'(r) \leq r\chi'(r) + s\chi'(s). \tag{45}$$

Now, we introduce the functions ξ and ζ defined for all $t \geq 0$ by

$$\rho_1(t) = \int_\Omega \chi(u_\mu^+ - u_\mu(t))dx, \quad \rho_2(t) = \int_\Omega \chi(w_\mu^+ - w_\mu(t))dx.$$

Since $U_0(x) \in R_\mu = [0, u_\mu^+] \times [0, w_\mu^+]$ for all $x \in \Omega$, we have $\rho_1(0) = \rho_2(0) = 0$. Furthermore, since $\chi(s) \geq 0$ for all $s \in \mathbb{R}$, we have $\rho_1(t) \geq 0$ and $\rho_2(t) \geq 0$ for all $t > 0$. Since ρ_1 is continuously differentiable on $\mathbb{R}$, we obtain its time derivative

$$\begin{aligned}
\dot{\rho_1}(t) &= \int_\Omega \frac{\partial(u_\mu^+ - u_\mu(t))}{\partial t}\chi'(u_\mu^+ - u_\mu(t))dx \\
&= \alpha \int_\Omega (w_\mu^+ - w_\mu(t))\chi'(u_\mu^+ - u_\mu(t))dx - \int_\Omega [q_\mu(u_\mu^+) - q_\mu(u_\mu(t))]\chi'(u_\mu^+ - u_\mu(t))dx \\
&= \alpha \int_\Omega (w_\mu^+ - w_\mu(t))\chi'(u_\mu^+ - u_\mu(t))dx - \int_\Omega J_\mu(u_\mu^+, u_\mu(t))(u_\mu^+ - u_\mu(t))\chi'(u_\mu^+ - u_\mu(t))dx \\
&\leq \alpha \int_\Omega (w_\mu^+ - w_\mu(t))\chi'(u_\mu^+ - u_\mu(t))dx + 2J_\mu^*\rho_1(t)
\end{aligned}$$

by applying (44) and denoting that

$$J_\mu(u_\mu^+, u_\mu(t)) = \frac{q_\mu(u_\mu^+) - q_\mu(u_\mu(t))}{u_\mu^+ - u_\mu(t)}, \quad \forall t \geq 0.$$

It is obvious that $J_\mu(u_\mu^+, u_\mu(t))$ gives the coefficient of the line that joins the points of coordinates $(u_\mu^+, q_\mu(u_\mu^+))$ and $(u_\mu(t), q_\mu(u_\mu(t)))$ in the plane $\mathbb{R}^2$. Hence, there exists $J_\mu^* \geq 0$ such that

$$J_\mu(u_\mu^+, u_\mu(t)) \geq -J_\mu^*, \quad \forall t \geq 0.$$

In particular, if assumption (6) is satisfied, which ensures that $J_\mu(u_\mu^+, u_\mu(t))$ is positive, then we can easily erase the corresponding term in the above estimation.

In parallel, the time derivative of ρ_2 is given by

$$\begin{aligned}\dot{\rho_2}(t) &= \int_\Omega \frac{\partial(w_\mu^+ - w_\mu(t))}{\partial t}\chi'(w_\mu^+ - w_\mu(t))dx \\ &= \delta\int_\Omega \Delta(w_\mu^+ - w_\mu(t))\chi'(w_\mu^+ - w_\mu(t))dx + \alpha\int_\Omega (u_\mu^+ - u_\mu(t))\chi'(w_\mu^+ - w_\mu(t))dx \\ &\quad - \beta\int_\Omega (w_\mu^+ - w_\mu(t))\chi'(w_\mu^+ - w_\mu(t))dx \\ &\leq \alpha\int_\Omega (u_\mu^+ - u_\mu(t))\chi'(w_\mu^+ - w_\mu(t))dx\end{aligned}$$

by applying property (44) and the Green formula with the Neumann boundary condition, i.e., for all $t \geq 0$,

$$\int_\Omega \Delta(w_\mu^+ - w_\mu(t))\chi'(w_\mu^+ - w_\mu(t))dx = -\int_\Omega \left|\nabla(w_\mu^+ - w_\mu(t))\right|^2 dx \leq 0.$$

Eventually, for all $t \geq 0$, we have

$$\begin{aligned}\dot{\rho_1}(t) + \dot{\rho_2}(t) &\leq \alpha\int_\Omega (u_\mu^+ u_\mu(t))\chi'(w_\mu^+ w_\mu(t))dx + \alpha\int_\Omega (w_\mu^+ - w_\mu(t))\chi'(u_\mu^+ - u_\mu(t))dx + 2J_\mu^*\rho_1(t) \\ &\leq \alpha\int_\Omega (w_\mu^+ w_\mu(t))\chi'(w_\mu^+ w_\mu(t))dx + \alpha\int_\Omega (u_\mu^+ - u_\mu(t))\chi'(u_\mu^+ - u_\mu(t))dx + 2J_\mu^*\rho_1(t) \\ &\leq 2\alpha[\rho_1(t) + \rho_2(t)] + 2J_\mu^*\rho_1(t) \\ &\leq 2(\alpha + J_\mu^*)[\rho_1(t) + \rho_2(t)]\end{aligned}$$

by employing property (45). We then apply the Gronwall lemma to deduce that

$$\rho_1(t) + \rho_2(t) \leq [\rho_1(0) + \rho_2(0)]e^{2(\alpha + J_\mu^*)t} \leq 0, \quad \forall t \geq 0.$$

Owing to $\rho_1(0) = \rho_2(0) = 0$, we deduce that $\rho_1(t) + \rho_2(t) = 0$. Moreover, we have $\rho_1(t), \rho_2(t) \geq 0$, which yields that $\rho_1 = \rho_2 \equiv 0$. The proof is complete. □

Although the invariant region $\mathscr{R}_\mu$ defined by (42) depends on the perturbation parameter μ, we can prove the existence of a L^∞-bound for the dynamical system $S_\mu(t)$, which is uniform with respect to μ. Indeed, it suffices to remark that the homogeneous stationary solution (u_μ^+, w_μ^+) given by (12) that delimits $\mathscr{R}_\mu$ varies continuously with μ. Note that such a uniform bound could not be established for the absorbing set $\mathcal{B}_\mu$ derived from Theorem 1 (see Remark 2).

Corollary 1 (Uniform bound)**.** *There exists a positive constant $M_{\mathscr{R}}$ such that, for all $\mu \in [0, \mu_1]$ and for all $U_0 \in \mathscr{R}_\mu$:*

$$\|S_\mu(t)U_0\|_{L^\infty(\Omega)^2} \leq M_{\mathscr{R}}. \tag{46}$$

Proof. Let $\mu \in [0, \mu_1]$ and let $U_0 \in \mathscr{R}_\mu$. For $t \geq 0$, we denote $\big(u_\mu(t), w_\mu(t)\big) = S_\mu(t)U_0$. By virtue of Theorem 4, we have

$$|u_\mu(t)| \leq u_\mu^+, \quad |w_\mu(t)| \leq w_\mu^+, \quad \forall t \geq 0.$$

Next, it is easily seen that (u_μ^+, w_μ^+) depends continuously on μ. Hence we can consider

$$u_{\max}^+ = \max_{0\leq\mu\leq\mu_1} u_\mu^+, \quad w_{\max}^+ = \max_{0\leq\mu\leq\mu_1} w_\mu^+,$$

from which we deduce $|u_\mu(t)| \leq u_{\max}^+$ and $|w_\mu(t)| \leq w_{\max}^+$ for all $t \geq 0$ and for all $\mu \in [0, \mu_1]$. Finally, we introduce $M_{\mathscr{R}} = \max(u_{\max}^+, w_{\max}^+)$, which achieves the proof. □

4.2 Continuity of the flow and of the stationary solutions

In this section, we consider the perturbed dynamical system $S_\mu(t)$ determined by (9) with $\mu > 0$, and the unperturbed dynamical system $S_0(t)$ obtained with $\mu = 0$ in (9). The following theorem establishes the continuity of the flow $S_\mu(t)$ when μ tends to 0, and plays a significant role to prove the continuity of the stationary solutions.

Theorem 5 (Continuity of the flow)**.** *Suppose that assumption (6) holds. Suppose moreover that $\mathscr{R}_\mu \subset \mathscr{R}_0$ for all $\mu \in (0, \mu_1]$. Let $U_\mu(t) = (u_\mu, w_\mu)^\top$ and $U(t) = (u, w)^\top$ denote, respectively, the global solutions to the degenerate forest kinematic model (2) when $\mu > 0$ and $\mu = 0$. Then, there exists a positive constant $\varrho = \min\left\{\frac{q_0}{2}, \beta\right\}$, such that, for all $U_0 \in \mathscr{R}_\mu$ and all $t \geq 0$, the following estimate is fulfilled:*

$$\|S_\mu(t)U_0 - S_0(t)U_0\|_Y^2 \leq \frac{\mu^2 M_1^2 |\Omega|}{q_0(\alpha - \varrho)}(e^{2(\alpha-\varrho)t} - 1). \tag{47}$$

Moreover,

(i) if $\alpha - \varrho < 0$, then $U_\mu(t) \overset{\mu\to 0^+}{\longrightarrow} U(t)$ in Y uniformly for $t \in [0, +\infty)$;

(ii) if $\alpha - \varrho > 0$, then $U_\mu(t) \overset{\mu\to 0^+}{\longrightarrow} U(t)$ in Y uniformly in every compact interval $[0, T]$ with $T > 0$.

Proof. Let $\varphi = u_\mu - u$, $\psi = w_\mu - w$ and $\Psi(t) = (\varphi, \psi)^\top = U_\mu(t) - U(t)$, then we can rewrite the degenerate forest kinetic system as following

$$\begin{cases} \dfrac{\partial \varphi}{\partial t} = \alpha\psi - q_\mu(u_\mu) + q(u) & \text{in } (0, +\infty) \times \Omega, \\ \dfrac{\partial \psi}{\partial t} = \delta\Delta\psi - \beta\psi + \alpha\varphi & \text{in } (0, +\infty) \times \Omega, \\ \dfrac{\partial \psi}{\partial \nu} = 0 & \text{on } (0, +\infty) \times \Gamma, \\ \varphi(0, x) = \varphi_0(x),\ \psi(0, x) = \psi_0(x) & \text{in } \Omega. \end{cases} \tag{48}$$

Multiply the first equation of (48) by φ, and integrate the product in Ω to have

$$\frac{1}{2}\frac{d}{dt}\|\varphi\|_{L^2}^2 = \alpha \int_\Omega \varphi\psi dx - \int_\Omega (q_\mu(u_\mu) - q(u))\varphi dx,$$

we next multiply the second equation of (48) by ψ, and integrate the product in Ω to have

$$\frac{1}{2}\frac{d}{dt}\|\psi\|_{L^2}^2 = \delta \int_\Omega \Delta\psi \cdot \psi dx - \beta\|\psi\|_{L^2}^2 + \alpha \int_\Omega \varphi\psi dx.$$

Combine the above two equations to have

$$\frac{1}{2}\frac{d}{dt}\|\Psi\|_Y^2 = 2\alpha \int_\Omega \varphi\psi dx + \delta \int_\Omega \Delta\psi \cdot \psi dx - \beta\|\psi\|_{L^2}^2 - \int_\Omega (q_\mu(u_\mu) - q(u))\varphi dx.$$

Note that

$$2\alpha \int_\Omega \varphi\psi dx \leq \alpha\|\varphi\|_{L^2}^2 + \alpha\|\psi\|_{L^2}^2$$

by employing the Young's inequality, and

$$\delta \int_\Omega \Delta\psi \cdot \psi dx = -\delta\|\nabla\psi\|_{L^2}^2 \leq 0$$

by employing the Green formula with Neumann boundary conditions. Besides, owing to the properties of the potential $Q_\mu(u)$, $p(u)$, the L^p interpolation inequality, and the ϵ-Young's inequality we have

$$\begin{aligned} -\int_\Omega (q_\mu(u_\mu) - q(u))\varphi dx &= -\int_\Omega (q_\mu(u_\mu) - q_\mu(u))\varphi dx - \int_\Omega \mu p(u)\varphi dx \\ &\leq -q_0\|\varphi\|_{L^2}^2 + \mu M_1 \int_\Omega \varphi dx \\ &\leq -\frac{q_0}{2}\|\varphi\|_{L^2}^2 + \frac{\mu^2 M_1^2 |\Omega|}{2q_0}, \end{aligned}$$

by taking $\epsilon = \frac{q_0}{2}$. Then, it is derived from the above that

$$\frac{1}{2}\frac{d}{dt}\|\Psi\|_Y^2 \le \alpha\|\varphi\|_{L^2}^2 + \alpha\|\psi\|_{L^2}^2 - \beta\|\psi\|_{L^2}^2 - \frac{q_0}{2}\|\varphi\|_{L^2}^2 + \frac{\mu^2 M_1^2|\Omega|}{2q_0} \le (\alpha-\varrho)\|\Psi\|_Y^2 + \frac{\mu^2 M_1^2|\Omega|}{2q_0},$$

where $\varrho = \min\left\{\frac{q_0}{2}, \beta\right\}$, then it follows from the Gronwall lemma that

$$\|\Psi\|_Y^2 \le e^{2(\alpha-\varrho)t}\|\Psi_0\|_Y^2 + \frac{\mu^2 M_1^2|\Omega|}{q_0(\alpha-\varrho)}(e^{2(\alpha-\varrho)t}-1) \le \frac{\mu^2 M_1^2|\Omega|}{q_0(\alpha-\varrho)}(e^{2(\alpha-\varrho)t}-1).$$

Furthermore, if $\alpha - \varrho < 0$, it is obvious that there exists a positive constant ε small enough so that

$$\|U_\mu(t) - U(t)\|_Y \le \frac{\varepsilon}{3} = \sqrt{\frac{2\mu^2 M_1^2|\Omega|}{q_0(\alpha-\varrho)}}, \quad \mu \to 0^+.$$

Similarly, if $\alpha - \varrho > 0$, then there exists $C_{\mu,t} > 0$ depending on μ and t so that

$$\|U_\mu(t) - U(t)\|_Y \le C_{\mu,t} = \sqrt{\frac{\mu^2 M_1^2|\Omega|}{q_0(\alpha-\varrho)}(e^{2(\alpha-\varrho)t}-1)}, \quad \mu \to 0^+,\ t \in [0,T],\ T > 0.$$

The proof is complete. □

By virtue of case (i) in Theorem 5, the following main result can be deduced.

Theorem 6 (Continuity of the stationary solutions)**.** *Suppose that the assumptions in Theorem 5 hold. Let $\bar{U}_\mu, \bar{U}$ be the stationary solutions to the forest kinematic model (2) when $\mu > 0$ and $\mu = 0$ respectively. Then, if $\alpha - \varrho < 0$, we have $\bar{U}_\mu \xrightarrow{\mu\to 0} \bar{U}$ in Y.*

Proof. It follows from Theorem 2 that $U_\mu(t) \to \bar{U}_\mu$ in Y as $t \to \infty$, i.e., for $\mu \in (0, \mu_1]$, there exists $\varepsilon > 0$ so that

$$\|U_\mu(t) - \bar{U}_\mu\|_Y \le \frac{\varepsilon}{3}.$$

In parallel, when $\mu = 0$, Theorem 2 still holds as long as the assumption $c - \frac{1}{3}ab^2 \ge 0$ is satisfied, i.e., $U(t) \to \bar{U}$ in Y as $t \to \infty$. Thus, we have $\|U(t) - \bar{U}\|_Y \le \frac{\varepsilon}{3}$. Combine with the conclusion in case (i) of Theorem 5 , we eventually deduce that

$$\|\bar{U}_\mu - \bar{U}\|_Y \le \|\bar{U}_\mu - U_\mu(t)\|_Y + \|U_\mu(t) - U(t)\|_Y + \|U(t) - \bar{U}\|_Y \le \varepsilon, \quad \mu \to 0^+, t \to \infty,$$

which completes the proof. □

Remark 5. *Note that we can not conclude that $\bar{U}_\mu \xrightarrow{\mu\to 0^+} \bar{U}$ in Y when $\alpha - \varrho > 0$. Due to the assertion in case (ii) of Theorem 5, the dissipative estimation (47) only holds on a compact time interval $[0,T]$. In particular, the above convergence results and continuity estimations are based on the assumption that $Q_\mu(u)$ is convex.*

Remark 6 (Extension of Theorem 3)**.** *We can apply Theorem 6 in order to extend the parameter domain of validity of the Computer Assisted Theorem 3. Indeed, we can deduce that the probability for a global solution of system (2) to converge to a non-constant stationary solution is positive for the parameters values given in Theorem 3, but with a parameter perturbation $\mu > 0$ small enough.*

4.3 A robust family of weak attractors

Numerous results on the effect of a perturbation on the asymptotic behavior of a given dynamical system have been established. Very often, these results express a type of robustness of the global attractor [7, 9, 14, 27, 37], whereas results on the robustness of ω-limit sets are rare [8]. More specifically, robustness is often described by proving the upper or lower semi-continuity of the global attractor with respect to the perturbation parameter.

As mentioned previously, compactness is a necessary requirement for proving such statements [28]. Here, the compactness requirement is not fulfilled. However, we can still prove that the set $\mathscr{A}_\mu$ defined by

$$\mathscr{A}_\mu = \overline{\bigcup_{U_0 \in \mathscr{R}_\mu} \omega_Y^\mu(U_0)}^Y, \quad \mu > 0, \tag{49}$$

where the set $\omega_Y^\mu(U_0)$ is given by (41), attracts the trajectories of the forest kinematic model (2) and varies smoothly with μ. Recall that the distance in Y between a element $u \in Y$ and a bounded set $B \subset Y$ is defined as $d_Y(u, B) = \inf_{v \in B} d_Y(u, v)$, and the semi-distance in Y between two bounded sets $B_1, B_2 \subset Y$ is defined by $d_Y(B_1, B_2) = \sup_{u \in B_1} d_Y(u, B_2)$.

Theorem 7 (A robust family of weak attractors)**.** *Suppose that assumption (6) holds. Suppose moreover that $\mathscr{R}_\mu \subset \mathscr{R}_0$ for all $\mu \in (0, \mu_1]$. Then the set $\mathscr{A}_\mu$ defined by (49) satisfies the following properties:*

(i) $\mathscr{A}_\mu$ is invariant, closed and uniformly bounded in Y, for all $\mu \in (0, \mu_1]$;

(ii) $\mathscr{A}_\mu$ attracts in Y the trajectories of (2) starting in $\mathscr{R}_\mu$, for all $\mu \in (0, \mu_1]$, that is:

$$\lim_{t \to +\infty} d_Y\big(S_\mu(t)U_0, \mathscr{A}_\mu\big) = 0, \tag{50}$$

for all $U_0 \in \mathscr{R}_\mu$ and for all $\mu \in (0, \mu_1]$;

(iii) if $\alpha - \varrho < 0$, then the family $\{\mathscr{A}_\mu\}_{0<\mu\leq\mu_1}$ satisfies

$$d_Y\big(\mathscr{A}_\mu, \mathscr{A}_0\big) \leq C\mu, \tag{51}$$

where C is a positive constant and $\varrho = \min\big\{\frac{q_0}{2}, \beta\big\}$.

Proof. (i) Let $\mu \in (0, \mu_1]$. It follows from the definition (49) that $\mathscr{A}_\mu$ is invariant and closed in Y. Next, let $U_\mu \in \mathscr{A}_\mu$. Then there exists a sequence $(U_{\mu,n})$ in $\bigcup_{U_0 \in \mathscr{R}_\mu} \omega_Y^\mu(U_0)$ such that $(U_{\mu,n})$ converges to U_μ in Y as n tends to $+\infty$. By virtue of Theorem 2, we have $\omega_Y^\mu(U_0) = \{\ell^\mu(U_0)\}$, for each $U_0 \in \mathscr{R}_\mu$, where we shortly denote by $\ell^\mu(U_0)$ the limit in Y of the trajectory $S_\mu(t)U_0$. Hence, we have $U_{\mu,n} = \ell^\mu(U_{\mu,n,0})$ for each $n \geq 0$, with $U_{\mu,n,0} \in \mathscr{R}_\mu$. Now, Corollary 1 guarantees that $\|S_\mu(t)U_{\mu,n,0}\|_Y \leq \widetilde{M}_{\mathscr{R}}$ for all $t \geq 0$, where $\widetilde{M}_{\mathscr{R}}$ is a positive constant that does not depend on μ. We can deduce that $\|U_{\mu,n}\|_Y \leq \widetilde{M}_{\mathscr{R}}$ for all $n \geq 0$, and finally that $\|U_\mu\|_Y \leq \widetilde{M}_{\mathscr{R}}$, for all $U_\mu \in \mathscr{A}_\mu$ and for all μ, which proves that $\mathscr{A}_\mu$ is uniformly bounded in Y.

(ii) Let $U_0 \in \mathscr{R}_\mu$. Theorem 2 guarantees that $S_\mu(t)U_0$ converges in Y to $\ell^\mu(U_0)$ as t tends to $+\infty$, with $\omega_Y^\mu(U_0) = \{\ell^\mu(U_0)\}$, which can be written

$$\lim_{t \to +\infty} d_Y\big(S_\mu(t)U_0, \ell^\mu(U_0)\big) = 0.$$

But we have $d_Y\big(S_\mu(t)U_0, \mathscr{A}_\mu\big) \leq d_Y\big(S_\mu(t)U_0, \ell^\mu(U_0)\big)$, since $\ell^\mu(U_0) \in \mathscr{A}_\mu$, which proves (50).

(iii) Let $U_\mu \in \mathscr{A}_\mu$. We consider again a sequence $(U_{\mu,n})$ in $\bigcup_{U_0 \in \mathscr{R}_\mu} \omega_Y^\mu(U_0)$ such that $(U_{\mu,n})$ converges to U_μ in Y as n tends to $+\infty$, and we write again $U_{\mu,n} = \ell^\mu(U_{\mu,n,0})$ with $U_{\mu,n,0} \in \mathscr{R}_\mu$. Now, we have

$$d_Y(U_{\mu,n}, \mathscr{A}_0) = d_Y\big(\ell^\mu(U_{\mu,n,0}), \mathscr{A}_0\big) \leq d_Y\big(\ell^\mu(U_{\mu,n,0}), \ell^0(U_{\mu,n,0})\big),$$

where $\ell^0(U_{\mu,n,0})$ denotes the limit in Y of the unperturbed trajectory $S_0(t)U_{\mu,n,0}$ (which is well defined, since $\mathscr{R}_\mu \subset \mathscr{R}_0$). Since $\alpha < \min\big\{\frac{q_0}{2}, \beta\big\}$, Theorem 5 ensures that

$$d_Y\big(\ell^\mu(U_{\mu,n,0}), \ell^0(U_{\mu,n,0})\big) \leq C\mu,$$

for all $\mu \in (0, \mu_1]$ and for all $n \geq 0$, with $C > 0$. We can deduce that $d_Y(U_{\mu,n}, \mathscr{A}_0) \leq C\mu$, for all $n \geq 0$ and consequently that $d_Y(U_\mu, \mathscr{A}_0) \leq C\mu$, for all $U_\mu \in \mathscr{A}_\mu$. We obtain $d_Y(\mathscr{A}_\mu, \mathscr{A}_0) \leq C\mu$, which proves (51). The proof is complete. □

Remark 7. *Theorem 7 guarantees that the set $\mathscr{A}_\mu$ defined by (49) attracts in Y the trajectories of the kinematic forest model (2). However, due to the lack of compactness, it is not known if the set $\mathscr{A}_\mu$ attracts the bounded sets of $\mathscr{R}_\mu$.*

4.4 Case of a strong perturbation

We end this section with the case of a strong perturbation, obtained for $\mu > \mu_2$ ($\mu_2 > \mu_1 > 0$). The following theorem proves that in this case, the orbits of the dynamical system (9) converge to the trivial equilibrium.

Theorem 8. *Let $\mu > \mu_2$, then there exists $\rho^* > 0$ such that for each $U_0 \in \mathcal{K}$, the solution $U_\mu(t)$ of the degenerate forest kinetic system (2) stemming from U_0 satisfies*

$$\|U_\mu(t)\|_Y \leq \|U_0\|_Y e^{-\rho^* t}, \quad t \geq 0.$$

Proof. Since $\mu > \mu_2$, there exists $\rho > 0$ such that $q_\mu(u) \geq \left(\frac{\alpha^2}{\beta} + \rho\right) u$ if $u \geq 0$ and $q_\mu(u) \leq \left(\frac{\alpha^2}{\beta} + \rho\right) u$ if $u \leq 0$. Hence we have $uq_\mu(u) \geq (\frac{\alpha^2}{\beta} + \rho)u^2$, for all $u \in \mathbb{R}$. Now we introduce the energy function L defined for $t \geq 0$ by

$$L(t) = \frac{1}{2} \int_\Omega [u_\mu^2(t) + w_\mu^2(t)] dx,$$

which is continuously differentiable. We easily show the estimate

$$\dot{L}(t) \leq 2\alpha \int_\Omega u_\mu(t) w_\mu(t) dx - \left(\frac{\alpha^2}{\beta} + \rho\right) \int_\Omega u_\mu^2(t) dx - \beta \int_\Omega w_\mu^2(t) dx$$

by applying the Green formula with the Neumann boundary and the assumption above. Now we apply the generalized Young's inequality to write

$$2\alpha \int_\Omega u_\mu(t) w_\mu(t) dx \leq \frac{\alpha}{\varepsilon} \int_\Omega u_\mu^2(t) dx + \alpha\varepsilon \int_\Omega w_\mu^2(t) dx,$$

in which we can choose a proper $\varepsilon > 0$ to ensure $\frac{\alpha}{\varepsilon} = \frac{\alpha^2}{\beta} + \frac{\rho}{2}$, i.e., $\varepsilon = \dfrac{\alpha}{\frac{\alpha^2}{\beta} + \frac{\rho}{2}}$. Therefore, we obtain

$$\dot{L}(t) \leq -\frac{\rho}{2} \int_\Omega u_\mu^2(t) dx - (\beta - \alpha\varepsilon) \int_\Omega w_\mu^2(t) dx,$$

where $\beta - \alpha\varepsilon > 0$ is guaranteed by the choice of ε. Note that $\rho^* = \min\{\rho, \beta - \alpha\varepsilon\}$, we thus obtain that $\dot{L}(t) \leq -\rho^* L(t)$. Employing again the Gronwall lemma, we complete the proof. □

5 Numerical simulations illustrating ecological properties

In this section, we aim to illustrate with relevant numerical simulations the theoretical results established above, and to show how the perturbed forest kinetic model (2) fulfills various ecological properties of interest. Firstly, we experiment the effect of several perturbations on the position of the *ecotone*, which corresponds to the frontier between the forest and another ecosystem (as for instance savanna in tropical regions, or tundra in boreal regions). These perturbations are expected to model the impact of global warming on the biological dynamics of the ecosystem. However, as the complex mechanisms of global warming are not yet precisely understood, we experiment several functions for the perturbation $p(u)$ involved in (3), mainly determined by polynomial or sinusoidal expressions. Then, we present numerical results that prove that the forest kinetic model (2) can reproduce the formation of chaotic patterns [29].

As in Section 3.4, our numerical computations were performed using a Strang type splitting scheme [36], with a finite elements discretization in space, and a Runge-Kutta method in time. The computation code was again executed in a GNU/LINUX environment, with the free software FreeFem++ [15]. For all simulations, we have considered an elliptic domain Ω of width $L = 500$ and height $\ell = 300$; we have again fixed the parameters of the forest kinetic model (2) as $\alpha = \beta = 1$, $\delta = 10$, $a = 0.6$, $b = 1$, $c = 0.9$. With these parameters, the unperturbed problem admits three homogeneous equilibrium states given by $O = (0, 0)$, $U^- = (1 - \frac{1}{\sqrt{6}}, 1 - \frac{1}{\sqrt{6}})$ and $U^+ = (1 + \frac{1}{\sqrt{6}}, 1 + \frac{1}{\sqrt{6}})$.

5.1 Shift of the ecotone or modification of the persistence equilibrium

One of the most fascinating properties of forest ecosystems is their ability to migrate in space, while they are obviously populations of sedentary individuals. Recently, it has been proved in [2] that this indirect diffusion, when combined with a hysteresis process, can explain the separation of trajectories, that reproduces the formation of an ecotone (see [30]). As forest ecosystems are highly destabilized by climatic and anthropic perturbations, it is relevant to investigate the impact of a perturbation on the position of the ecotone. In the ecological science literature, it is well described that the ecotone can be simply shifted to the north or to the south, depending on the nature of the perturbation and on the geographical region, or can be highly modified and exhibit the formation of chaotic or fractal patterns [40]. For instance, in [11], a northward shift is proved to occur in the boreal forest-tundra ecotone; in [31], the tropical forest-savanna ecotone is studied and it is shown that climate change can modify the trees density near the ecotone; in [33], island tropical montane cloud forests are studied and it is observed that climate change might push them towards higher elevations.

Here, to reproduce these complex mechanisms, we consider two shift perturbations s_1, s_2 defined by

$$s_1(u) = auu^-(u-u^+), \qquad s_2(u) = -auu^-(u-u^+). \tag{52}$$

The effect of these shift perturbations on the cubic function $q(u)$ is depicted in Figure 1: when μ increases, the persistence equilibrium U_μ^+ is not modified, thus can be denoted U^+. However, the saddle equilibrium U_μ^- is shifted to the left under the action of $s_1(u)$, or to the right under the action of $s_2(u)$. The shift can also be visualized on the energy levels of the potential $H_\mu(u,w)$ defined by (2.2), as illustrated in Figure 2.

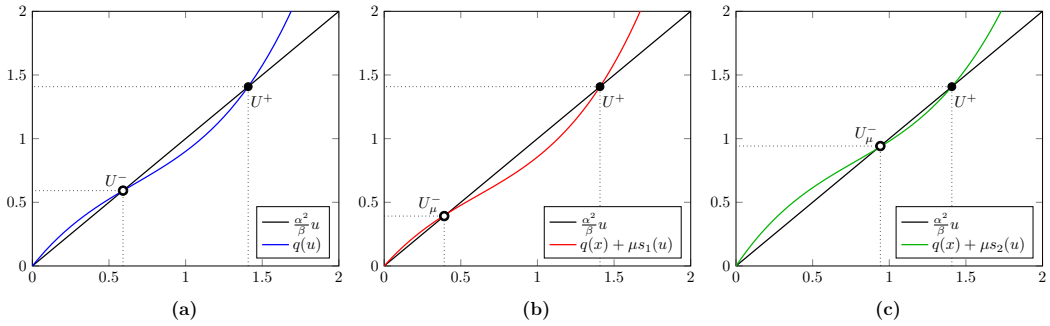

Figure 1: *Effect of the shift perturbations $s_1(u)$, $s_2(u)$ defined by (52) on the cubic function $q(u)$.* ***(a)*** *Shape of the unperturbed cubic function $q(u)$.* ***(b)*** *When μ increases, the persistence equilibrium $U_\mu^+ = U^+$ is not modified; the saddle equilibrium U_μ^- is shifted to the left under the action of $s_1(u)$.* ***(c)*** *The saddle equilibrium U_μ^- is shifted to the right under the action of $s_2(u)$.*

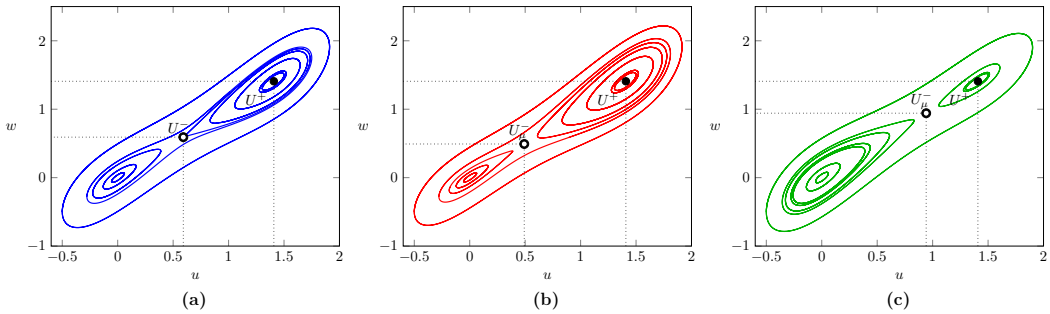

Figure 2: *Effect of the shift perturbations $s_1(u)$, $s_2(u)$ defined by (52) on the energy levels of the potential $H_\mu(u,w)$ defined by (2.2).* ***(a)*** *Energy levels of the unperturbed potential.* ***(b)*** *Under the action of $s_1(u)$, the saddle U_μ^- is shifted to the left, whereas the persistence equilibrium $U_\mu^+ = U^+$ is not modified.* ***(c)*** *Under the action of $s_2(u)$, the saddle U_μ^- is shifted to the right.*

Next, we have considered an initial condition $\big(u_0(x), w_0(x)\big)$ which is equally distributed within the basins of attraction of the extinction equilibrium O and of the persistence equilibrium U_μ^+. As proved in [3], the trajectory of the forest kinetic model (2) starting from such an initial condition is expected to converge to

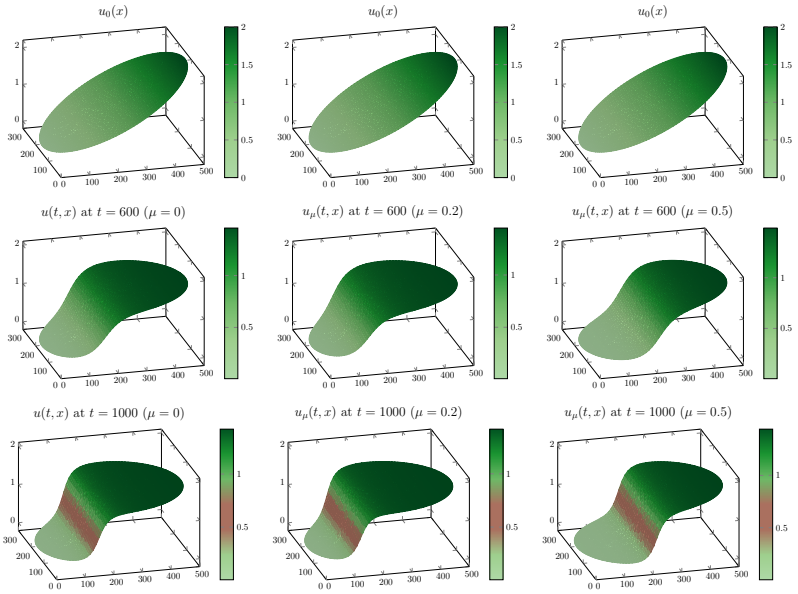

Figure 3: *Numerical simulation showing the effect of the shift perturbations $s_1(u)$, $s_2(u)$ on the position of the ecotone. In the last row, the position of the ecotone is highlighted by a brown band. Under the action of $s_1(u)$, the ecotone is shifted to the left (second column). Under the action of $s_2(u)$, it is shifted to the right (third column).*

a heterogeneous stationary solution that reproduces the ecotone. Hence, we have computed the trajectories $\big(u(t,x), w(t,x)\big)$, $\big(u_\mu(t,x), w_\mu(t,x)\big)$, of the unperturbed problem and of the problem perturbed by $s_1(u)$ or $s_2(u)$, respectively. The results are depicted in Figure 3, where we focus on the density of trees. In this figure, the color semantics is chosen according to intuition: deep green illustrates a high density of trees, while pale green represents a low density of trees. We have chosen a 3D view in order to visualize the formation of the ecotone. In the first column, we show the time evolution of the trees density $u(t,x)$ of the unperturbed trajectory, from $t = 0$ (at the top), until $t = 1000$ (at the bottom). In the second and third columns, we show the time evolution of the trees density $u_\mu(t,x)$ of the trajectories perturbed by $s_1(u)$ and $s_2(u)$, respectively. In the asymptotic phase ($t = 1000$), the ecotone is highlighted by a brown band, located at the position of the domain Ω where the density of trees decreases very rapidly. As expected, the ecotone is shifted to the left under the action of $s_1(u)$, which implies that the area occupied by the high density of trees spreads in the domain Ω. If the perturbation parameter μ is increased, the area occupied by a high density of trees can even invade the whole domain Ω. At the opposite, the ecotone is shifted to the right under the action of $s_2(u)$, which implies that the area occupied by a high density of trees shrinks. Hence, these numerical simulations show that the perturbed forest model (2) can faithfully reproduce ecological observations of great interest.

Afterwards, we have also experimented two perturbations m_1, m_2 that are expected to modify the persistence equilibrium U_μ^+, without impacting the position of the ecotone. The perturbations m_1, m_2 are defined by the polynomial expressions

$$m_1(u) = auu^+(u-u^-), \qquad m_2(u) = -auu^+(u-u^-). \tag{53}$$

The effects of the perturbations $m_1(u)$, $m_2(u)$ on the cubic function $q(u)$ and on the energy levels of the potential $H(u,w)$ are depicted in Figures 4 and 5, respectively. Under the action of the perturbation $m_1(u)$, the persistence equilibrium U_μ^+ is decreased, whereas it is increased under the action of the perturbation $m_2(u)$. In parallel, the saddle point U_μ^- is not modified, thus can be denoted U^-.

With the perturbations $m_1(u)$, $m_2(u)$ defined by (53), we have again considered an initial condition $\big(u_0(x), w_0(x)\big)$ which is equally distributed within the basins of attraction of the extinction equilibrium O and of the persistence equilibrium U_μ^+. The perturbed trajectories starting from that initial condition are depicted in Figure 6. We observe that the trajectory behaves as expected, with a modification of the level of the persistence equilibrium U_μ^+ and no modification of the position of the ecotone. It is worth noting that this behavior reproduces a non trivial ecological transition which is well observed and described: indeed, under the action of climate change, forest ecosystems can exhibit a deep modification of their dynamics, such as, for instance, the savannization of the Amazon forest (see e.g. [35]), that leads to a sharp fall of the density of trees in the ecosystem.

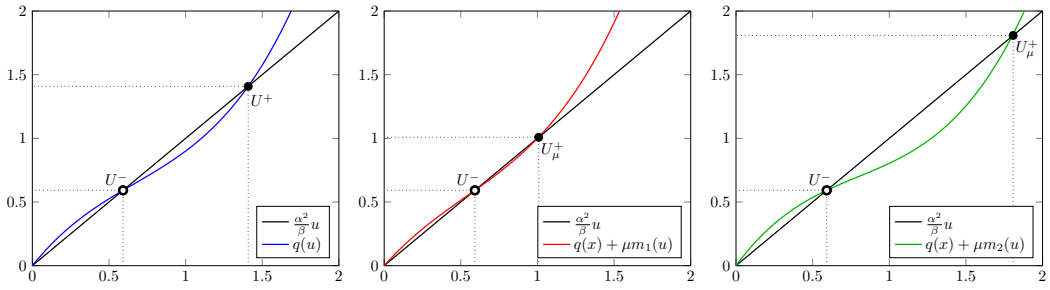

Figure 4: *Effect of the perturbations $m_1(u)$, $m_2(u)$ defined by (53) on the cubic function $q(u)$. **(a)** Shape of the unperturbed cubic function $q(u)$. **(b)** The persistence equilibrium U_μ^+ decreases under the action of $m_1(u)$. **(c)** It increases under the action of $m_2(u)$. In parallel, the saddle point $U_\mu^- = U^-$ is not modified.*

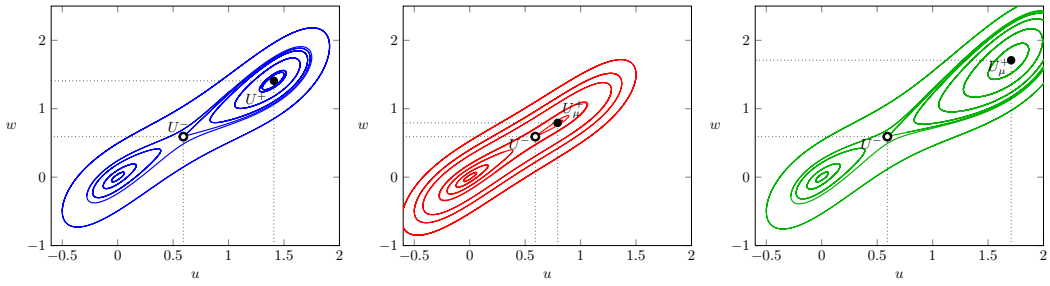

Figure 5: *Effect of the perturbations $m_1(u)$, $m_2(u)$ defined by (53) on the energy levels of the potential $H_\mu(u,w)$. **(a)** Energy levels of the unperturbed potential. **(b)** The persistence equilibrium U_μ^+ decreases under the action of $m_1(u)$. **(c)** It increases under the action of $m_2(u)$.*

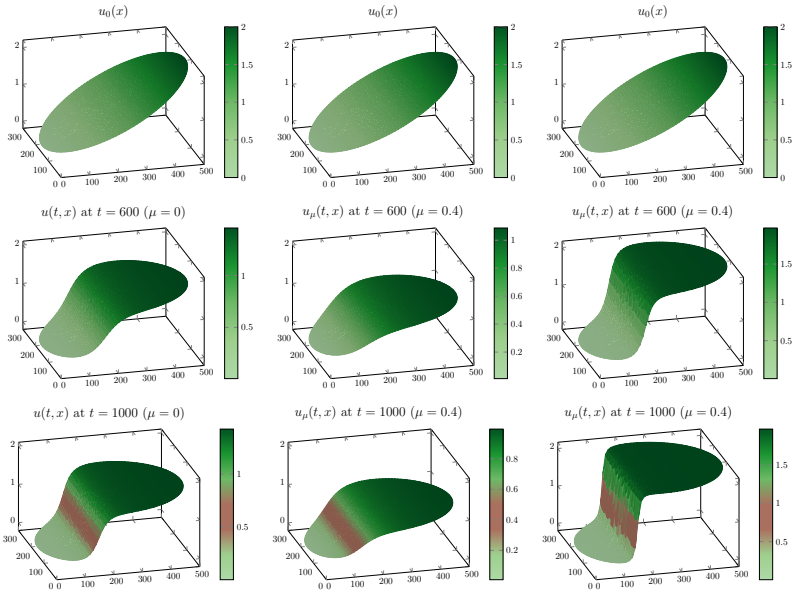

Figure 6: *Numerical simulation showing the effect of the perturbations $m_1(u)$, $m_2(u)$ on the level of the persistence equilibrium U_μ^+. In the last row, the position of the ecotone is again highlighted by a brown band. Under the action of $m_1(u)$, the level of persistence is decreased (second column). Under the action of $m_2(u)$, it is increased (third column). In parallel, the position of the ecotone is not varied.*

5.2 Emergence of intermediate ecosystems

We continue with numerical simulations of the forest kinematic model (2) perturbed by a periodic process. Hence, we consider the perturbations $p_1(u)$, $p_2(u)$ and $p_3(u)$ defined by

$$p_1(u) = \sin(20u), \qquad p_2(u) = \sin(9u), \qquad p_3(u) = \sin(11u). \tag{54}$$

The effects of the perturbations $p_1(u)$, $p_2(u)$ and $p_3(u)$ are depicted in Figures 7 and 8, with $\mu = 0.035$, $\mu = 0.09$ and $\mu = 0.07$, respectively. Note that these values of the perturbation parameter μ guarantee that the perturbed cubic function $q_\mu(u)$ is still monotone; however, it admits more than three intersection points with the line $w = \frac{\alpha^2}{\beta}u$. These supplementary intersection points are expected to perturb the form and the position of the ecotone. In parallel, the positions of the intersection points can modify the values of the trees density at equilibrium.

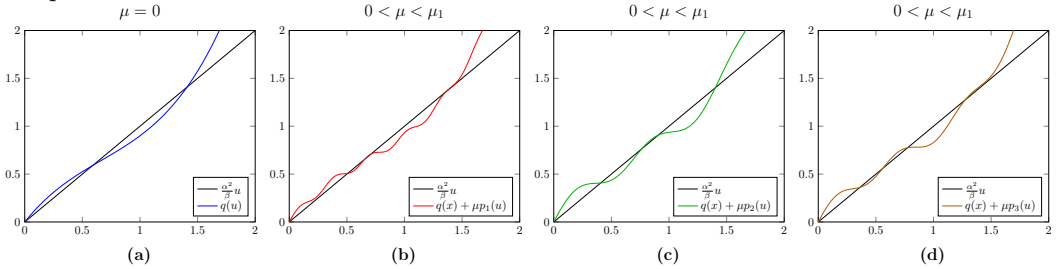

Figure 7: Effect of the perturbations $p_1(u)$, $p_2(u)$, $p_3(u)$ defined by (54) on the cubic function $q(u)$. **(a)** Shape of the unperturbed cubic function $q(u)$. **(b)-(c)-(d)** The perturbed function $q_\mu(u)$ admits more than three intersection points with the line $w = \frac{\alpha^2}{\beta}u$.

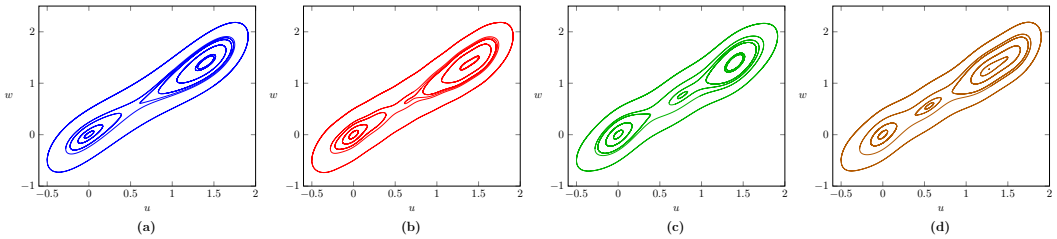

Figure 8: *Effect of the perturbations $p_1(u)$, $p_2(u)$, $p_3(u)$ defined by (54) on the energy levels of the potential $H(u, w)$. **(a)** Energy levels of the unperturbed potential $H(u, w)$. **(b)-(c)-(d)** The perturbed potential $H_\mu(u, w)$ admits a supplementary saddle point and a supplementary sink.*

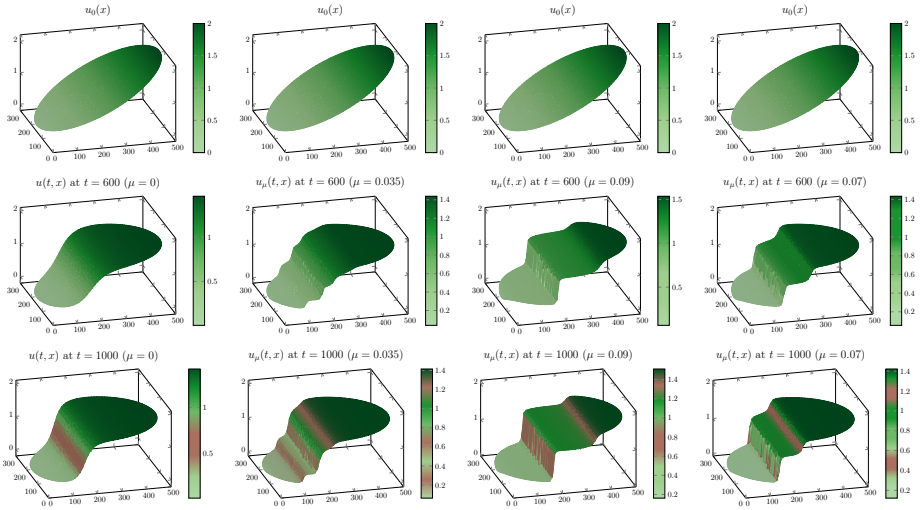

Figure 9: *Numerical simulation showing the effect of the periodic perturbations $p_1(u)$, $p_2(u)$, $p_3(u)$ on the dynamics of the forest model (2). In the last row, the positions of the ecotones are highlighted by brown bands. Under the action of the perturbations, the form of the ecotone is modified and intermediate ecosystems emerge. The size and trees densities of these intermediate ecosystems are very sensitive to the nature of the perturbation.*

With the perturbations $p_1(u)$, $p_2(u)$, $p_3(u)$ defined by (54), we have again considered an initial condition $\big(u_0(x), w_0(x)\big)$ which is equally distributed within the basins of attraction of the extinction equilibrium O and of the persistence equilibrium U_μ^+. The perturbed trajectories starting from that initial condition are depicted in Figure 9. In this figure, we show the time evolution of the density of trees $u_\mu(t,x)$ for each perturbation. We observe that the position and the form of the ecotone are modified and intermediate ecosystems emerge. The size and trees densities of these intermediate ecosystems are very sensitive to the intensity and the nature of the perturbation. In each case, the perturbation leads to a decrease of the total living biomass, which is in concordance with ecological observations (see for instance [13]).

5.3 Randomly generated initial conditions lead to chaotic patterns

We end this section with numerical simulations of the forest kinetic model (2), starting from randomly generated initial conditions. We have chosen an initial condition $\big(u_0(x), w_0(x)\big)$, $x \in \Omega$, using the random number generator `randreal()` of the FreeFem++ software, and we have computed two trajectories of the forest kinetic model (2). The first trajectory $\big(u(t,x), w(t,x)\big)$ is the solution of the unperturbed problem (that is, with $\mu = 0$), while the second trajectory $\big(u_\mu(t,x), w_\mu(t,x)\big)$ is the solution of the perturbed problem, with $p(u) = \sin(20u)$ and $\mu = 0.035$.

Our results are presented in Figure 10. In this figure, the left column shows the time evolution of the density of trees $u(t,x)$ (of the unperturbed trajectory), from $t = 0$ (at the top), until $t = 2000$ (at the bottom). The color semantics is the same as in Figures 3 and 6 (deep green models a high density of trees, and pale green corresponds to a low density of trees). However, we have chosen a map view rather than a 3D view, so as to better visualize the formation of patterns. The second column shows the time evolution of the density of trees $u_\mu(t,x)$ (of the perturbed trajectory), with the same color semantics. The third and fourth columns show the time evolution of the densities of seeds $w(t,x)$ and $w_\mu(t,x)$ (unperturbed and perturbed trajectories, respectively); white and yellow correspond to a high density of seeds, while blue and brown model a low density of seeds.

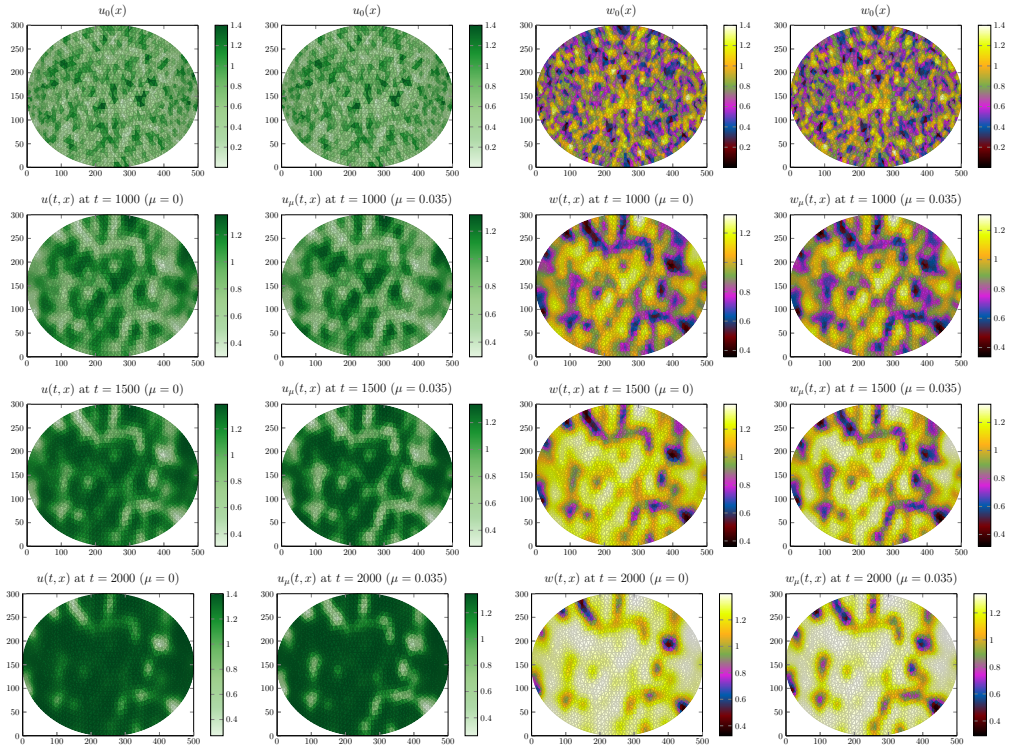

Figure 10: *Numerical simulation showing the time evolution of the densities of trees $u(t,x)$, $u_\mu(t,x)$ (first and second columns) and of the densities of seeds $w(t,x)$, $w_\mu(t,x)$ (third and fourth columns), corresponding to an unperturbed trajectory and a perturbed trajectory of the forest kinetic model (2), respectively. Starting from a randomly generated initial condition, the trajectories converge to a stationary solution that exhibits spots patterns with a low density of trees and seeds.*

We observe that the trajectories converge to a heterogeneous stationary solution that exhibits spots patterns with a low density of trees and seeds. For instance, a white spot of low density of trees is located at the position $(400, 200)$ of the domain Ω (first and second columns, at the bottom), in correspondence with a brown spot of low density of seeds, located at the same position (third and fourth columns, at the bottom). According to Theorem 7, the stationary solution is robust with respect to a variation of the perturbation parameter μ, that is, the spots are smoothly modified by an increase of μ. Hence, modifications of the spots can be identified after a careful look, but these modifications are small. However, these spots are very sensitive a change of the initial condition $\big(u_0(x), w_0(x)\big)$. Indeed, we show in Figure 11 the limits of two other trajectories $\big(u(t,x), w(t,x)\big)$, $\big(u_\mu(t,x), w_\mu(t,x)\big)$, starting from another randomly generated initial condition $\big(u_0(x), w_0(x)\big)$. As in Figure 10, we observe the formation of spots, modeling a low density of trees and seeds. While these spots are again smoothly modified by the perturbation parameter μ, their number and location are completely different in Figures 10 and 11. Therefore, these patterns admit a chaotic behavior. It is worth emphasizing that such a chaotic behavior has been intensely studied in non degenerate reaction-diffusion systems admitting a diffusion driven instability (see notably [29] and the references therein); however, chaotic patterns emerging in degenerate reaction-diffusion systems as the forest model (2) have not been as much analyzed. In particular, given an initial condition $\big(u_0(x), w_0(x)\big)$, it seems very difficult to predict the position of spots of the corresponding trajectory.

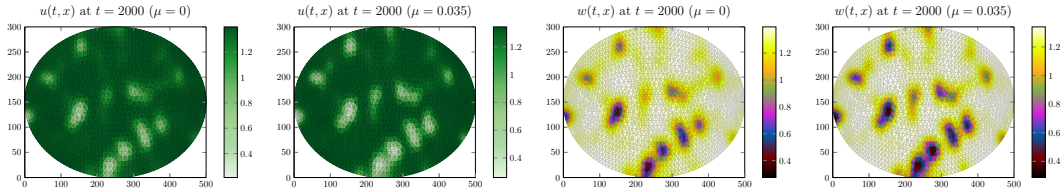

Figure 11: *Numerical simulation showing the limits of two trajectories* $\big(u(t,x), w(t,x)\big)$, $\big(u_\mu(t,x), w_\mu(t,x)\big)$ *starting from another randomly generated initial condition* $\big(u_0(x), w_0(x)\big)$. *The trajectories converge to a stationary solution that again exhibits spots patterns with a low density of trees and seeds. However, the number and location of spots are completely different than in Figure 10.*

6 Conclusion

In this paper, we studied the dynamics of a perturbed forest kinematic model (2). We firstly presented the preliminary results. Then, we established the asymptotic convergence result by proving that the Lyapunov function generated by the system satisfies the Łojasiewicz-Simon gradient inequality, which is guaranteed by the monotonicity of the nonlinear perturbation $q_\mu(u)$, i.e. when assumption (6) holds. Besides, we provided an original algorithm, based on the Monte-Carlo method, to further clarify the convergence result. Furthermore, we established the existence of a family of positively invariant regions for the dynamical system $\{S_\mu(t)\}$, and proved the continuity of the flow, which yields the continuity of the stationary solutions. We finally addressed the robustness of the weak attractors, which is highly nontrivial. However, when the monotonicity assumption is violated, no rigorous result can be obatined. We also presented the case of a strong perturbation, which leads to trivial dynamics. At last but not the least, we performed numerical simulations to better understand the forest ecosystem. We showed the modification of the persistence equilibrium, and the emergence of intermediate ecosystems associated with different perturbations. We also introduced the chaotic patterns caused by randomly generated initial conditions.

Acknowledgment. This research is part of the project "*Stability and resilience of the Amazonian forest socio-ecosystem in the face of climatic and anthropogenic disturbances*" supported by the IMPT (Institute of Mathematics for Planet Earth) of the CNRS (French National Centre for Scientific Research). Besides, the authors express their sincere gratitude to Professor Alain Miranville for useful comments and warm encouragements on this work.

References

[1] D. Aronson, A. Tesei, and H. Weinberger. A density-dependent diffusion system with stable discontinuous stationary solutions. *Annali di Matematica Pura ed Applicata*, 152:259–280, 1988.

[2] G. Cantin. Non-existence of the global attractor for a partly dissipative reaction-diffusion system with hysteresis. *Journal of Differential Equations*, 299:333–361, 2021.

[3] G. Cantin. How hysteresis produces discontinuous patterns in degenerate reaction–diffusion systems. *Asymptotic Analysis*, pages 1–16, 2022.

[4] G. Cantin. On the robustness of discontinuous patterns in degenerate reaction–diffusion systems with perturbed hysteresis. *Communications in Nonlinear Science and Numerical Simulation*, 131:107842, 2024.

[5] G. Cantin, B. Delahaye, and B. M. Funatsu. On the degradation of forest ecosystems by extreme events: Statistical model checking of a hybrid model. *Ecological Complexity*, 53:101039, 2023.

[6] G. Cantin, A. Ducrot, and B. M. Funatsu. Mathematical modeling of forest ecosystems by a reaction–diffusion–advection system: impacts of climate change and deforestation. *Journal of Mathematical Biology*, 83(6):1–45, 2021.

[7] T. Caraballo, J. A. Langa, and J. C. Robinson. Upper semicontinuity of attractors for small random perturbations of dynamical systems. *Communications in Partial Differential Equations*, 23(9-10):1557–1581, 1998.

[8] H. Cui, P. E. Kloeden, and M. Yang. Forward omega limit sets of nonautonomous dynamical systems. *Discrete Contin. Dyn. Syst. Ser. B*, 13:1103–1114, 2019.

[9] M. Efendiev and A. Yagi. Continuous dependence on a parameter of exponential attractors for chemotaxis-growth system. *Journal of the Mathematical Society of Japan*, 57(1):167–181, 2005.

[10] M. Efendiev and S. Zelik. Global attractor and stabilization for a coupled pde-ode system. pages 1–23. arXiv:1110.1837v1, 2011.

[11] P. Evans and C. D. Brown. The boreal–temperate forest ecotone response to climate change. *Environmental Reviews*, 25(4):423–431, 2017.

[12] E. Feireisl and F. Simondon. Convergence for semilinear degenerate parabolic equations in several space dimensions. *J. Dynam. Differential Equations*, 12(3):647–673, 2000.

[13] D. Galbraith, P. E. Levy, S. Sitch, C. Huntingford, P. Cox, M. Williams, and P. Meir. Multiple mechanisms of Amazonian forest biomass losses in three dynamic global vegetation models under climate change. *New Phytologist*, 187(3):647–665, 2010.

[14] J. K. Hale and G. Raugel. Upper semicontinuity of the attractor for a singularly perturbed hyperbolic equation. *Journal of Differential Equations*, 73(2):197–214, 1988.

[15] F. Hecht. New development in FreeFem++. *Journal of numerical mathematics*, 20(3-4):251–266, 2012.

[16] T. Hérault, R. Lassaigne, F. Magniette, and S. Peyronnet. Approximate probabilistic model checking. In *International Workshop on Verification, Model Checking, and Abstract Interpretation*, pages 73–84. Springer, 2004.

[17] S. Iwasaki. Asymptotic convergence of solutions to the forest kinematic model. *Nonlinear Analysis: Real World Applications*, 62:103382, 2021.

[18] A. Köthe, A. Marciniak-Czochra, and I. Takagi. Hysteresis-driven pattern formation in reaction-diffusion-ODE systems. *Discrete and Continuous Dynamical Systems*, 40(6):3595, 2020.

[19] D. J. Krieger. Economic value of forest ecosystem services: a review. 2001.

[20] Y. A. Kuznetsov, M. Y. Antonovsky, V. Biktashev, and E. Aponina. A cross-diffusion model of forest boundary dynamics. *Journal of Mathematical Biology*, 32(3):219–232, 1994.

[21] C. Le Huy, T. Tsujikawa, and A. Yagi. Stationary solutions to forest kinematic model. *Glasgow Mathematical Journal*, 51(1):1–17, 2009.

[22] R. Le Roux et al. How wildfres increase sensitivity of Amazon forests to droughts. *Environ. Res. Lett.*, 17:044031, 2022.

[23] A. Legay, B. Delahaye, and S. Bensalem. Statistical model checking: An overview. In *International conference on runtime verification*, pages 122–135. Springer, 2010.

[24] S. Łojasiewicz. Une propriété topologique des sous-ensembles analytiques réels. *Proc. Colloques internationaux du C.N.R.S: Les équations aux dérivées partielles*, 117:87–89, 1963.

[25] A. Marciniak-Czochra and M. Kimmel. Reaction–diffusion approach to modeling of the spread of early tumors along linear or tubular structures. *Journal of Theoretical Biology*, 244(3):375–387, 2007.

[26] M. Mimura. Stationary pattern of some density-dependent diffusion system with competitive dynamics. *Hiroshima Mathematical Journal*, 11(3):621–635, 1981.

[27] A. Miranville and S. Zelik. Attractors for dissipative partial differential equations in bounded and unbounded domains. *Handbook of differential equations: evolutionary equations*, 4:103–200, 2008.

[28] I. Moise, R. Rosa, and X. Wang. Attractors for non-compact semigroups via energy equations. *Nonlinearity*, 11(5):1369, 1998.

[29] J. D. Murray. *Mathematical Biology: II: Spatial Models and Biomedical Applications*, volume 3. Springer, 2003.

[30] R. P. Neilson. Transient ecotone response to climatic change: some conceptual and modelling approaches. *Ecological applications*, 3(3):385–395, 1993.

[31] F. B. Passos, B. S. Marimon, O. L. Phillips, P. S. Morandi, E. C. das Neves, F. Elias, S. M. Reis, B. de Oliveira, T. R. Feldpausch, and B. H. Marimon Junior. Savanna turning into forest: concerted vegetation change at the ecotone between the Amazon and Cerrado biomes. *Brazilian Journal of Botany*, 41:611–619, 2018.

[32] C. A. Peres, J. Barlow, and W. F. Laurance. Detecting anthropogenic disturbance in tropical forests. *Trends in ecology & evolution*, 21(5):227–229, 2006.

[33] R. Pouteau, T. W. Giambelluca, C. Ah-Peng, and J.-Y. Meyer. Will climate change shift the lower ecotone of tropical montane cloud forests upwards on islands? *Journal of Biogeography*, 45(6):1326–1333, 2018.

[34] M. Renardy and R. C. Rogers. *An Introduction to Partial Differential Equations, second ed.* Springer-Verlag, New York, 2004.

[35] D. V. Silvério, P. M. Brando, J. K. Balch, F. E. Putz, D. C. Nepstad, C. Oliveira-Santos, and M. M. Bustamante. Testing the Amazon savannization hypothesis: fire effects on invasion of a neotropical forest by native cerrado and exotic pasture grasses. *Philosophical Transactions of the Royal Society B: Biological Sciences*, 368(1619):20120427, 2013.

[36] G. Strang. On the construction and comparison of difference schemes. *SIAM Journal on Numerical Analysis*, 5(3):506–517, 1968.

[37] R. Temam. *Infinite-dimensional dynamical systems in mechanics and physics*, volume 68. Springer Science & Business Media, 2012.

[38] A. Yagi. *Abstract parabolic evolution equations and their applications*. Springer Science & Business Media, 2009.

[39] E. Zeidler. *Nonlinear Functional Analysis and its Applications I: Fixed-Point Theorems*. Springer-Verlag, New York, 1986.

[40] Y. Zeng and G. P. Malanson. Endogenous fractal dynamics at alpine treeline ecotones. *Geographical Analysis*, 38(3):271–287, 2006.